

Author's Comments (AC)

Manuscript: amt-2017-419

Manuscript title: Characterization of a catalyst-based total nitrogen and carbon conversion technique to calibrate particle mass measurement instrumentation

Response to Reviewers:

The following discussion includes the reproduced text from the reviewer (bold), along with our detailed responses and the corresponding changes (italics; eliminated text is struck through) made to the revised manuscript. All page and line numbers refer to the original manuscript.

We thank both Referees for their thorough comments and constructive suggestions, which were helpful in improving the manuscript. We have addressed their issues and concerns to the best of our ability.

Anonymous Referee #1

In this well written manuscript, the authors present the characterization of a catalyst based total nitrogen and carbon conversion technique to calibrate particle mass measurement instrumentation, as clearly reflected in the title of the manuscript. Set-up, methodology, and conversion efficiencies for particle-bound nitrogen species are thoroughly discussed. The authors convincingly describe, that the instrument is capable of quantitatively converting a range of particle-bound nitrogen species and provides an online signal of total reactive nitrogen from both gas- and particle-phase, which is very useful for the assessment of nitrogen cycling in the atmosphere. The conversion of particle-bound carbon via a platinum catalyst is described for a number of organic compounds in laboratory-generated aerosols, while an application to the atmosphere remains challenging due to the small signal compared to background CO₂. Nevertheless, a simultaneous detection of total reactive nitrogen and total carbon in one instrumental set-up is a promising perspective. However, the organization of the manuscripts' content could be improved to increase the value of the paper. For example, clearly dividing the subjects instrument characterization (instrument set-up and experiment design, gas-phase Nr conversion efficiency, particle-phase Nr conversion efficiency, particle-phase C conversion efficiency, proof of concept - Nr measurements of biomass burning), and particle mass measurement calibration (laboratory generated aerosols, comparison with PILS-ESI/MS) in sections 2 and 3. A reader could then very quickly see why this new instrument is worth learning about. After addressing content organization and the specific comments listed below, the paper will be very well suited for publication in AMT.

We appreciate the Reviewer's positive comments, and agree that the manuscript could be reorganized to clarify the experimental approach, motivation, and conclusions. We have divided the manuscript into the following sections: (1) Introduction; (2) Experimental details including (a) instrument descriptions with an added total carbon (Cy) section; (b) experimental design, which includes an added section on methods for determining gas phase conversion efficiency per Reviewer 2's suggestion. The section "particle generation, measurement and characterization" was renamed "methods for determining particle phase conversion efficiency" and a few sentences were added or removed for organizational clarity within this section. (3) Instrument characterization, including both gas and particle conversion efficiency discussions and our "proof of concept" biomass burning emissions measurements; The section discussing the N_r-particle conversion efficiency was divided into two subsections (a) Challenges using the DMA/SMPS to determine N_r-particle conversion efficiency and (b) Determining N_r-particle conversion efficiency using a DMA and UHSAS. (4) Application to calibrate the PILS-ESI/MS using comparisons with the PiLS-ESI/MS (5) Summary and Conclusions. Sentences throughout the manuscript were occasionally shifted to a new section (see for e.g. the new total carbon (Cy) system section in the experimental details section now incorporates sentences originally included in the results section) or to a more appropriate section to improve the organization as suggested by the Reviewer. While these organizational changes added to the value of this paper, the pages, lines, and a few figure numbers were altered

from the original manuscript. As a result the following changes/discussion following the Reviewer's specific comments will continue to refer to the original manuscript.

The following section was added to the Experimental details:

"Total carbon (C_T) system

Measurements of total carbon (C_T) were accomplished by catalytic conversion to carbon dioxide (CO₂) and detection using a CO₂ analyzer. The high-temperature (750°C), platinum catalyst (Fig. 1) in the N_r system should quantitatively convert carbon containing species to CO₂ in the presence of air. Gas-phase carbon conversion across similar precious metals has been studied extensively (see for example the Pt catalyst used in Veres et al., 2010). The total flow through the Pt catalyst was set to ~1.5 standard L min⁻¹ and was then split before the MoOx catalyst. In our sampling scheme 0.5 sL min⁻¹ of flow was directed to a LICOR 6251 (LI-6251; Lincoln, NE) CO₂ analyzer, while the remaining flow, 1 sL min⁻¹, was directed through the MoOx catalyst and to the NO-O₃ chemiluminescence detector as detailed in Sect. 2.1.1. Run in this manner, the conversion of compounds that contain both N and C atoms can then be measured simultaneously using the NO-O₃ chemiluminescence detector and LI-6251 detector in parallel.

The LICOR instrument was internally referenced to scrubbed zero air. At ambient CO₂ levels, it is challenging to retrieve reliable measurements since the signal relative to the background abundance of CO₂ is small. In order to evaluate organic carbon conversion efficiency, our approach relies on using ultra-pure air for aerosol generation and carrier gas flow, therefore ambient CO and CO₂ is eliminated. The LI-6251 was calibrated with sub-5 ppm CO₂ standards (Scott-Marin Inc., Riverside, CA) in ultra-pure air. Due to the low signals levels and the uncertainty of the low concentration CO₂ standards, the overall uncertainty of the CO₂ measurements below 1 ppmv presented in this work is ± 10% for 10 second averages."

Specific comments:

1. Could you think of a more representative name or acronym for your instrument? The term N_r instrument does not totally reflect the purpose of the instrument in my opinion

While we appreciate the Reviewer's suggestion to create an alternate acronym this is primarily an instrument for on-line measurement of gas- and particle-phase total reactive nitrogen. We explicitly state in the introduction that the converter coupled with the NO-O₃ chemiluminescence detection is referred to as the "N_r system." For the purposes of organic carbon measurements we direct the sample stream following the heated platinum catalyst to an off-board NDIR CO₂ detector and there are additional sampling restrictions since the small signal compared to background CO₂ limits ambient sampling. When we discuss organic carbon conversion specifically, we highlight that the method of conversion is across the platinum catalyst only, which is the front-end of our "N_r system." We have also added a subsection to the instrument descriptions section to specifically detail the total carbon measurement approach. Additionally, future experiments will focus on quantifying sulfur conversion followed by SO₂ detection and we wish to hold off on naming the complete nitrogen/carbon/sulfur instrument until it is fully characterized.

2. Please include more recent references on P. 2 L. 6, e.g., Jimenez, et al. 2009, Science; Hallquist et al. 2010, ACP; etc.

The Reviewer was right to point out that we have not included more recent publications or reviews, thus we have added the two references suggested to the appropriate paragraph.

P2 L7 Added text: “Jimenez et al., 2009; Hallquist et al., 2010”

P19 L10 Added reference: “Hallquist, M., Wenger, J. C., Baltensperger, U., Rudich, Y., Simpson, D., Claeys, M., Dommen, J., Donahue, N. M., George, C., Goldstein, A. H., Hamilton, J. F., Herrmann, H., Hoffmann, T., Iinuma, Y., Jang, M., Jenkin, M. E., Jimenez, J. L., Kiendler-Scharr, A., Maenhaut, W., McFiggans, G., Mentel, Th. F., Monod, A., Prévôt, A. S. H., Seinfeld, J. H., Surratt, J. D., Szmigielski, R., and Wildt, J.: The formation, properties and impact of secondary organic aerosol: current and emerging issues, *Atmos. Chem. Phys.*, 9, 5155-5236, <https://doi.org/10.5194/acp-9-5155-2009>, 2009.”

3. You sometimes speak of “these experiments” or “these studies” in the manuscript, please consider revising these statements for clarity and readability

We thank the reviewer for their suggestion and agree that using the phrases “these experiments” and “these studies” are confusing and unnecessary, so we have revised the manuscript in several places by eliminating these phrases as follows:

P4 L11-12 Existing text: “The primary objective of these experiments is to characterize particle conversion” New text: “The primary objectives are to characterize particle conversion”

P4 L34 Existing text: “The operation of this instrument during these experiments often required considerable de-tuning to keep the instrument count rates below the roll-over point of the photon counting electronics (approximately 5 MHz), thus the detection limit was closer to 0.1 ppbv for these measurements.” New text: “The operation of this instrument often required considerable de-tuning to keep the instrument count rates below the roll-over point of the photon counting electronics (approximately 5 MHz) for the particle concentrations generated, thus the detection limit was closer to 0.1 ppbv (corresponding to 0.3 $\mu\text{g m}^{-3}$ for aerosol nitrate).”

P5 L27 Existing text: “A detailed description of the PILS used in these studies can be found” New text: “A detailed description of the PILS can be found”

P12 L33 Existing text: “The inorganic salts selected for this study” New text: “The inorganic salts selected for the comparison between N_r and the PILS-ESI/MS instruments”

P15 L13 Existing text: “The N_r - particles tested in these experiments span the” New text: “The N_r - particles tested span the”

4. The purpose of the MoOx catalyst, i.e., reducing NO₂ to NO, is not clearly stated in section 2.1

We have added the following sentence:

P4 L31-32 “The heated MoOx catalyst reduces the remaining NO₂ to NO.”

5. Please carefully check through the manuscript again and try to revise extensive and anecdotic paragraphs for conciseness. Exemplarily, please have a look at lines 6 – 29 on page 7 and revise this paragraph.

While we have edited the suggested paragraph, we feel the information that was not eliminated from the paragraph is important and the organizational changes detailed earlier and completed per Reviewer 1's suggestion more clearly supports their inclusion. The specific revised text is indicated below:

P7 L6-29 Existing text: "In these experiments particle diameters from 100 to 600 nm were selected and the multiply-charged particles in the size distribution were accounted for as described below. For the liquid concentrations and atomizer conditions we used, the DMA output size distribution is a multi-peaked population consisting not only of singly charged particles but also particles with multiple (mostly two or three) charges. The multiply charged particles can contribute significantly to the overall mass and must be considered when calculating particle mass. The distributions of singly, doubly, and triply charged particles can vary depending on the solution concentration. We measured atomized size distributions using the scanning mobility particle sizer (SMPS; Wang and Flagan, 1990) function of the DMA (physical diameter, $D_p = 1\text{-}1000$ nm). The DMA transfer theory (Knutson and Whitby, 1975; Stolzenburg, 1988) with Wiedensohler's (1988) steady-state charge distribution approximation was used to estimate the fraction of multiply charged particles contributing to the CPC number concentration for each diameter setting. There are a number of possible sources of uncertainty using these methods that may include particle losses, DMA transfer function uncertainty, counting uncertainty, and inversion errors. Consequently, the size distribution of particles selected at a particular voltage and flow setting of the DMA was examined using the UHSAS. UHSAS particle sizing is a function of the amount of light scattered onto the photodetectors. The quantity of scattered light, however, depends not only on the particle size, but also on the composition-dependent particle refractive index (Bohren and Huffman, 1983; Liu and Daum, 2000; Hand and Kreidenweis 2002; Rosenberg et al., 2012). The UHSAS manufacturer recommended calibration uses PSL microspheres, which are well characterized and have known refractive index ($n = 1.58$) and shape. Because the UHSAS sizing is sensitive to particle refractive index, a new sizing calibration curve was produced for each studied particle type (i.e. refractive index) (Kupc et al., 2017). Considering this, we used the DMA, with sizing accuracy $\sim \pm 2.5\%$ and NIST-traceable PSLs for 150 –500 nm spheres as our calibration standard. The UHSAS sizing was recalibrated by using the DMA to select particles of known size for each of the aerosol types studied. A different UHSAS calibration curve was produced and used for each aerosol type (e.g. Kupc et al., 2017). These calibration curves were used to retrieve accurate particle size distributions so that the multiply charged particles were properly accounted for. "

New text: "*For the liquid concentrations, atomizer conditions, and DMA settings used here, the DMA output size distribution was a multi-peaked population consisting not only of singly charged particles but also particles with multiple (mostly two or three) charges that can contribute significantly to the overall particle mass. Hence the particle mass could not be calculated directly from the singly-charged mobility diameter, particle density, and the CPC number concentrations. We generally used two methods to calculate the particle mass concentrations for these experiments. For the first method, the size distributions were measured using the scanning mobility particle sizer (SMPS; Wang and Flagan, 1990) function of the DMA (physical diameter, $D_p = 1\text{-}1000$ nm). We used the DMA transfer theory (Knutson and Whitby, 1975; Stolzenburg, 1988) with Wiedensohler's (1988) steady-state charge distribution approximation to estimate the fraction of multiply charged particles contributing to the CPC number concentration for each diameter setting. There are a number of possible sources of uncertainty using these methods that may include*

particle losses, DMA transfer function uncertainty, counting uncertainty, and inversion errors. When comparing mass concentrations from the SMPS with those measured by the N_r system, issues with the SMPS-derived size distributions became apparent (discussed separately in Section 3.2.2). For the second method of calculating mass concentrations, we directly measured the diluted, DMA output using the UHSAS. UHSAS particle sizing is a function of the amount of light scattered onto the photodetectors, which depends not only on the particle size, but also on the composition-dependent particle refractive index (Bohren and Huffman, 1983; Liu and Daum, 2000; Hand and Kreidenweis 2002; Rosenberg et al., 2012). The UHSAS manufacturer recommended calibration uses PSL microspheres, which are well characterized and have known refractive index ($n = 1.58$) and shape. Because the UHSAS sizing is sensitive to particle refractive index, a new sizing calibration curve was produced for each studied particle type (i.e. refractive index) using a DMA to select particles for a range of known sizes (Kupc et al., 2018). These calibration curves were used to retrieve accurate particle size distributions that properly accounted for the multiply charged particles. “

The following are additional areas of revised text:

P3 L17 We have eliminated the following text as it is repetitive: “~~By these methods, Roberts et al. (1998) confirmed efficient conversion of C1–C7 gas-phase compounds across the catalyst.~~”

P3 L30 We have eliminated the following text: “~~While these instrument calibration techniques are well-established for controlled laboratory-generated aerosol standards,~~”

P4 L10-11 Existing text: “a particle-into-liquid sampler coupled directly to an electrospray ionization source and by the N_r instrument.” New text: “~~the PILS-ESI/MS with that measured by the N_r instrument.~~”

P6 L15-16 We eliminated the following text: “~~For purposes of this comparison, matrix effects were assumed to be negligible for tests sampling single-component aerosols.~~”

P7 L35-37 We eliminated the following text: “~~For these reasons, we used the UHSAS size distributions to estimate the fraction of singly, doubly, and triply charged particles together with the total particle number taken from the CPC measurement to exclusive particle mass from total volume and density.~~” Then we added the following text to the end of the paragraph: “Due to problems with measuring SMPS size distributions and requiring coincidence corrections for the UHSAS number concentrations, we used the UHSAS size distributions with the total particle number taken from the CPC measurement to calculate particle mass from total volume and density.”

P10 L10-12 We eliminated the following text: “~~However, our results demonstrate the added challenges in particle mass determination using estimated size distributions from the SMPS method.~~”

P10 L12 We eliminated the following text: “~~Other aerosol measurement techniques (e.g. the Particle Time of Flight mode of the Aerosol Mass Spectrometer; DeCarlo et al., 2006) directly measure size distributions or instead measure polydisperse aerosol and the instrument and inversion algorithm corrections required using the SMPS are avoided~~”

And eliminate P18 L8-10: “~~DeCarlo, P. F., Kimmel, J. R., Trimborn, A., Northway, M. J., Jayne, J. T., Aiken, A. C., Gonin, M., Fuhrer, K., Horvath, T., Docherty, K. S., Worsnop, D. R., and Jimenez, J. L.: Field-deployable, high resolution, time-of-flight aerosol mass spectrometer, Anal. Chem, 78, 8281–8289, doi:10.1021/ac061249n, 2006.~~”

P12 L6-7 Existing text: “for the range of oxidation states. We are confident these results extend to other N_r -containing particles, which is supported by the extensive list of N_r gases efficiently converted as shown in Table 1. Therefore, we” New text: “for the range of oxidation states and should extend to other N_r -containing particles, we”

P 12 L18-20 We have eliminated the following text: “~~Initial tests with $(NH_4)_2C_2O_4$ proved more challenging as the low C number required large polydisperse aerosol loadings (several ppmv) to be measured reliably by the LICOR. During these instances, surface effects reduced the total N_r signal, which likely resulted from NH_3 scavenging to the walls of the transfer lines or quartz tubing.~~” And we combined the remaining sentences following this eliminated text with the above paragraph.

P12 L27-30 Existing text: “Here we demonstrate the capability of the total nitrogen system as an independent calibration method for aerosol measurement systems. N_r measurements of laboratory generated single-component inorganic and organic aerosol particles were used to characterize a novel configuration coupling a PILS with electrospray ionization interface followed by mass spectrometric detection.” New text: “Here we demonstrate the capability of the total nitrogen system as an independent calibration method for other aerosol measurement systems. N_r measurements of laboratory generated single-component inorganic and organic aerosol particles were used to characterize the PILS-ESI/MS.”

P12 L30-32 Existing text: “The strength of using the N_r system to calibrate the PILS-ESI/MS is that it is a direct method to calibrate the entire coupled on-line system. The current calibration approach involves liquid-phase standards to calibrate the ESI/MS independently from the PILS.” New text: “The strength of using the N_r system to calibrate the PILS-ESI/MS and other aerosol mass instruments is that it is a direct method to calibrate the entire coupled on-line system. The current calibration approach for nearly all detectors used with the PILS involves liquid-phase standards to calibrate the detection method independently from the PILS.”

P13 L6 We have eliminated the following text: “~~In coupling an aerosol collection technique (PILS) with an electrospray ionization source, water-soluble aerosol particles are speciated in real time.~~”

P13 L15-17 We have eliminated the following text: “~~Because a greater aerosol particle mass could be realized by directly sampling the polydisperse output of the atomizer, our analysis focuses on comparisons between N_r and PILS-ESI/MS without using the DMA size selection.~~”

P14 L30-32 We have eliminated the text: “~~We evaluated this previously uncharacterized mass measurement technique using both traditional particle number size distribution measuring systems and the total N_r mass measurement system.~~” And added text “Here” to begin the following sentence.

P14 L33-35 We have eliminated the following text: “~~Calibrating the ESI/MS using direct injection of liquid standards combined with mass concentrations collected by the PILS is a valid approach for quantifying inorganic components of aerosols, which likely extends to several organics as demonstrated by oxalate.~~”

P15 L2 to P14 L32 We moved the following sentence to an earlier section of the paragraph: “PILS characterization has been limited to theoretical predictions or experimental comparisons that involve coupling the PILS with a mass analyzer (e.g. IC; Orsini et al., 2003; Sorooshian et al., 2006).” And we added transition text: “In general,”

1 P15 L 3-5 We have eliminated the following text: ~~“Here we introduced a new method for calibrating the entire PILS-~~
2 ~~ESI/MS-coupled system using N_x -equivalent mass measurements of Cl^- , NO_3^- , SO_4^{2-} , $C_2O_4^{2-}$ from N_x -containing~~
3 ~~particles.”~~

4 P14 L35 We moved the following sentence to an earlier section of the paragraph, existing text: “However, these
5 ESI/MS calibrations are sensitive to the experimental conditions, which must be precisely maintained during ESI
6 calibrations and throughout the entire sampling period. Changes in flow rate, interface positioning, or solvent
7 composition have significant impacts on both the transmission and ionization efficiency ultimately effecting pre-
8 determined ESI calibration factors.” New text: *“However, our current ESI/MS calibration methods are sensitive to*
9 *the experimental conditions, which must be precisely maintained during ESI calibrations and throughout the entire*
10 *sampling period. Changes in flow rate, interface positioning, or solvent composition have significant impacts on both*
11 *the transmission and ionization efficiency ultimately effecting pre-determined ESI calibration factors.”*

12 **Exemplary technical comments:**

13 **P. 4, L. 3 should read “mass spectrometric detection”**

14 P4 L3 We added text: “*spectrometric*” between “mass” and “detection”

15 **P. 12, L. 20: should read “transfer lines”**

16 P12 L20 We have changed the existing text: “liens” New text: “*lines*”

17 **P. 13, L. 18: should read “Conventionally, : :”**

18 P13 L18 We added a comma “,” following “Conventionally”

19 **and other small mistakes, which should be considered upon revision of the manuscript**

20 There were a few other minor mistakes suggested by Reviewer 2 that we have corrected. Please refer to our response
21 to Reviewer 2 for a few additional corrections. We have included below other small mistakes we have revised in the
22 manuscript.

23 P2 L27 Existing text: “O₃” New text “*ozone (O₃)*”

24 P3 L22 Existing text: “specifications” New text: “*design*”

25 P4 L4 Existing text: “calibrated using” New text: “*compared to the calibration obtained with*”

26 P5 L31 Existing text: “The PILS sample flow” New text: “*The PILS liquid outlet flow*”

27 P6 L28 Existing text: “atomization of” New text: “*atomizing*”

28 P6 L29 Existing text: “in a dry particle-free nitrogen flow” New text: “*in a dry particle-free nitrogen or zero air flow*”

29 P6 L29 We added the text: “*similar to the one reported by*”

30 P6 L31 We added the text: “*similar to one described by*”

31 P6 L33 We eliminated the text: “~~*monodisperse*~~”

- 1 P7 L1 We added a comma. Existing text: “output flow following dilution” New text “*output flow, following dilution*”
- 2 P7 L1 Existing text: “We measured the flow ” New text: “*We measured the CPC flow rate*”
- 3 P7 L37 Existing text: “exclusive” New text: “*calculate*”
- 4 P9 L15 We inserted additional text: “*on rapid timescales (a few seconds)*” following “However, the total N_r response
- 5 precisely tracks the CPC signal”
- 6 P10 L14 Existing text: “Therefore, we instead” New text: “*Here we*”
- 7 P11 L1 Existing text: “ N_r measurements of biomass burning” New text: “ N_r measurement of biomass burning
- 8 emissions”
- 9 P11 L33 Existing text: “ambient air is eliminated” New text “*ambient CO and CO₂ is eliminated*”
- 10 P12 L21 Existing text: “ N_r system” New text: “ *N_r catalyst*”
- 11 P13 L3 Existing text: “measurements of nitrate” New text: “*measurements of ammonium salts of nitrate*”
- 12 P13 L7 Existing text: “through” New text: “*using*”
- 13 P15 L8 We eliminated the text “~~*monodisperse*~~”
- 14 P15 L31 Existing text: “demonstrated that this technique” New text: “*demonstrated that the N_r conversion technique*”
- 15 P15 L33 Existing text: “of” new text: “*within*”
- 16 P16 L28 We eliminated the text “~~*airborne*~~”
- 17 P17 L27 We capitalized the text: “aerodyne”
- 18 P18 L28 Existing text: “P. Natl. Acade.” New text: “*Proc. Natl. Acad.*”
- 19 P27 L4 Existing text: “commercial” New text: “*custom*”

J.Collett (Referee 2)

Stockwell et al. report a thorough and satisfying performance evaluation of a catalyst based approach to measuring particulate reactive N. Although others have explored similar approaches, the work has largely gone unpublished or lacked the thorough evaluation provided by the current authors. There is a compelling need to quantify total reactive N in airborne particles and I commend the authors for their efforts. I also commend them for the thoroughness of their evaluation and the care in which they describe limitations to their approach (e.g., the need to look at particulate OC in a CO₂-free stream, the importance of eliminating PILS-ESI-MS matrix/ion suppression effects by using single component standards, etc....). Their findings will be very useful to the broader atmospheric chemistry community, extending from those interested in source characterization to those interested in deposition and particle effects on human health and radiative scattering. I have a few suggestions for minor changes to improve the manuscript.

We thank Dr. Jeffrey Collett for his positive review and useful comments, which have added value to this paper. Additional specific responses are included below.

1. Title: I found the title confusing and somewhat misleading. The focus is primarily on N and primarily on direct measurement of particulate (or total) reactive N. The title should better reflect that.

We agree that it is important to straightforwardly describe the focus of this paper in the title. While we are characterizing a catalyst approach to quantitatively convert particulate nitrogen and organic carbon, we also believe it is important to present comparisons to other mass measurement systems as this may be of interest to scientists interested in alternate calibration approaches for their particle mass measurement systems. Thus, we have changed the title to better describe the manuscript

Existing title: "Characterization of a catalyst-based total nitrogen and carbon conversion technique to calibrate particle mass measurement instrumentation"

New title: "*Characterization of a catalyst-based conversion technique to measure total particulate nitrogen and organic carbon and comparison to a particle mass measurement instrument*"

2. Abstract: The mention of particulate organic carbon conversion in the abstract is, I suppose, appropriately brief. I do suggest that the authors here refer to "efficient" or "complete" conversion rather than simply conversion. I also suggest they point out here the important challenges of determining particulate OC by this method against a high concentration ambient background, as described in the manuscript itself.

We have added "efficient" before "conversion" and briefly describe this method's shortcomings for application to ambient sampling of particulate carbon.

P1 L24 We added text: "*efficient*" before "conversion"

P1 L25 We added new text to the abstract: "*However, the application of this method to the atmosphere presents a challenge due to the small signal above background at high ambient levels of common gas-phase carbon compounds (e.g. CO₂).*"

3. Section 3.1.1. The authors refer here to experimental methods not described in the methods section of the manuscript. I suggest an Experimental Details section be added on methods for checking gas-phase conversion efficiency. This would allow the authors to clearly convey information about calibration standards and comparison gas phase measurement methods. Section 3.1.1, for example, talks about apparent errors in the assumed ammonia absorption cross-section, but this is confusing because the reader has not been told how this is relevant to the gas-phase ammonia measurement method. The latter has not been specified.

We have added a section to more clearly describe the gas-phase conversion experiments. Per Reviewer 1's suggestions we have reorganized the manuscript, thus this new section was added to the "Experimental design" section prior to our discussion focusing on methods for determining particle phase conversion efficiency.

New added text/section:

"2.2.1 Methods for determining gas-phase conversion efficiency"

"The efficiency of conversion of several N-containing gases by the N_r catalyst was determined through addition of a number of representative compounds that were calibrated independently. The NO signal from the converted species was then compared to the signal from an NO in N_2 standard (5.38 ppmv, Scott-Marrin Inc., Riverside, CA) that was used as the working standard for this project. Typical calibration levels were in the range of 50 to 100 ppbv as determined by the mass flow controllers used to mix the standard into the measurement stream. The standards used for each compound and their associated calibrations were as follows.

The NO_2 standard stream was produced from the NO working standard through gas-phase titration with a small stream of O_2 in which O_3 had been produced by photolysis at 184.9 nm using a mercury discharge lamp. This technique is used routinely for NO_x and NO_y measurement systems (Williams et al., 1998) and allows straightforward determination of NO_2 conversion provided care is taken not to over-titrate the NO stream to produce NO_3 and therefore N_2O_5 . The uncertainty in the NO_2 conversion determination is simply the propagated errors in the subtraction of the signals before and after titration.

The ammonia (NH_3) conversion was examined using two different NH_3 sources, a gas mixture (3.1 ppmv in N_2 , Scott-Marrin) and a permeation device (Kin-Tek, LaMarque, Texas). Care was taken with these standards to keep them under flow for periods of several days in order to insure any system surfaces were equilibrated. The calibration of these standards was accomplished by ultraviolet (UV) absorption spectroscopy at 184.9 nm wavelength using an instrument described by Neuman et al, (2003), and based on absorption cross-sections reported in the literature (Tannenbaum et al., 1953; Lovejoy, 1999; Froyd, 2002). The uncertainty of NH_3 conversion was propagated based on the uncertainties in flow rate and UV absorption determinations.

The hydrogen cyanide (HCN) standard consisted of a commercial gravimetric mixture of HCN in N_2 (10 ppmv, GASCO Oldsmar, FL), which was mixed into the system using a mass flow controller. The specified uncertainty of this mixture was $\pm 10\%$, and the standard concentration was verified using long-path Fourier-transform infrared (FTIR) spectroscopy to within the stated uncertainty. The HCN standard was used to produce a gas phase stream of cyanogen chlorine (ClCN) by reaction with chloramine-T, a non-volatile chlorinating agent, which has been described previously (Valentour et al., 1974). To do this, a small stream (5 standard $cm^3\ min^{-1}$) of the HCN standard was combined with humidified Zero Air (ZA, 60% RH, 30 standard $cm^3\ min^{-1}$) over a bed packed with glass beads coated with a solution of chloramine-T. The glass beads were prepared by coating glass 3 mm outer diameter (OD) beads with a 2 g 100 mL^{-1} solution and packing $\sim 20\ cm^3$ of them in a 12.7 mm OD PFA tube and flowing ZA over them until dry. The reaction was shown to be essentially 100% ($\pm 10\%$) by proton-transfer reaction mass spectrometry (PTR-MS) when conducted in a humidified atmosphere ($RH \geq 60\%$), by FTIR analysis of the HCN and ClCN in the gas stream before and after chlorination.

The isocyanic acid (HNCO) standard was prepared according to the methods described by Roberts et al. (2010), in which the trimer, cyanuric acid, was thermally decomposed at 250°C in a diffusion cell to produce a steady stream of HNCO, which was then calibrated by long-path FTIR spectroscopy. Initially, this source has the potential to produce NH₃ as an impurity, most likely because of the presence of trace amounts of water. Keeping the source under flow and above 120°C at all times when not in use was found to reduce the NH₃ impurity to negligible levels (<5%), as measured by PTR-MS. The uncertainties in the HNCO standard were propagated from the uncertainties in the HNCO cross section (Northwest-Infrared, PNNL), the NH₃ subtraction, and flow rates. Standard streams of both nitrobenzene and trimethylamine were produced using gravimetrically prepared solutions and a commercial liquid calibration device (Ionicon, Innsbruck, Austria). The uncertainties in these liquid calibration standards were estimated from the propagated uncertainties in the solution concentrations and the liquid and gas flow rates

The conversion of nitrous oxide (N₂O) is a potential interference in the N_r method as N₂O is not typically considered a reactive nitrogen compound in the troposphere. Several experiments were conducted to determine the extent of this potential interference using a 10.1 ppmv N₂O standard. The resulting conversion efficiency ranged from 0.03% to 0.05% in dry and humidified air respectively. These can be considered upper limits for this interference as we cannot be completely sure that there were no N_r contaminants (e.g. NO₂) in the N₂O standard.”

We added the following references to accompany the above text:

P19 L3 Added text: “Froyd, K. D.: Ion induced nucleation in the atmosphere: Studies of ammonia, sulfuric acid, and water cluster ions, Ph.D., Department of Chemistry, University of Colorado, Boulder, Colorado, 282 pp., 2002.”

P21 L29 Added text: “Lovejoy, E. R.: Ion trap studies of H+(H₂SO₄)_m(H₂O)_n reactions with water, ammonia, and a variety of organic compounds, Int. J. Mass Spectrom., 190/191, 231-241, 1999.”

P25 L1 Added text: “Tannenbaum, E., Coffin, E. M., and Harrison, A. J.: The far ultraviolet absorption spectra of simple alkyl amines, J. Chem. Phys., 21, 311, doi: <https://doi.org/10.1063/1.1698878>, 1953.”

P8 L6-7 Existing text: “We verified the efficiency of conversion of a range of gas phase N_r compounds in this catalyst system using calibrated gas mixtures or standard streams and auxiliary analysis methods.” New text: “We verified the efficiency of conversion of a range of gas phase N_r compounds in this catalyst system using calibrated gas mixtures or standard streams and auxiliary analysis methods as described in Sect. 2.2.1.”

~~P8 L7-9 We eliminated the text: “We compared the total N_r signal measured as NO, where NO was calibrated using NO standards in nitrogen (Scott-Marrin Inc., Riverside, CA) to the known amount specified by the calibration method.”~~

P8 L11-12 Existing text: “The uncertainties in the measured conversion efficiencies encompass the propagated errors in each calibration method.” New text: “The uncertainties in the measured conversion efficiencies are the propagated errors in each calibration method, and in all cases the range encompasses 100 % conversion”

4. p. 8, line 29: It seems a bit odd here that the authors refer just to negligible interference from N₂O conversion in biomass burning sources. Why only discuss BB and not other (e.g., auto exhaust, ag, etc...) sources. The focus makes a bit more sense given later discussion about the Missoula FIREX experiment, but since this manuscript

1 is really addressing a more broadly applicable approach, it would be helpful to broaden the N₂O interference
2 discussion beyond BB

3 We have added the following text to extend the N₂O discussion to other sources so that biomass burning is not implied
4 as the only important source mentioned in the manuscript:

5 P8 L30 New text added: “N₂O emissions from other sources (e.g. natural and anthropogenic agricultural sources,
6 fossil fuel combustion, or animal waste) can be significant, therefore the interference from N₂O conversion must be
7 considered”

8 **5. top of p. 9: It is my sense that it is not so uncommon for NO concentrations to be in the range of 10s of pptv
9 in remote regions. I suggest the authors better justify or moderate their claim that an NO interference of 28
10 pptv is "clearly a negligible amount in almost any atmospheric context."**

11 The Reviewer raises a valid point here, which we address below.

12 P9 L1-2 Existing text: “an upper limit that is clearly a negligible amount in almost any atmospheric context” New
13 text: “an upper limit that is generally a negligible amount in almost any atmospheric context except in more remote
14 regions.”

15 **6. Section 3.1.4 and Fig. 6. This is an interesting timeline of deriving "excess" reactive N from the new
16 instrument measuring a smoke plume. Do the authors have a measurement of HNO₃ in the airstream? I suggest
17 that modified combustion efficiency (MCE) be added as a parameter in Fig. 6, if available, to help make the
18 authors' point re: periods of smoldering vs. flaming combustion.**

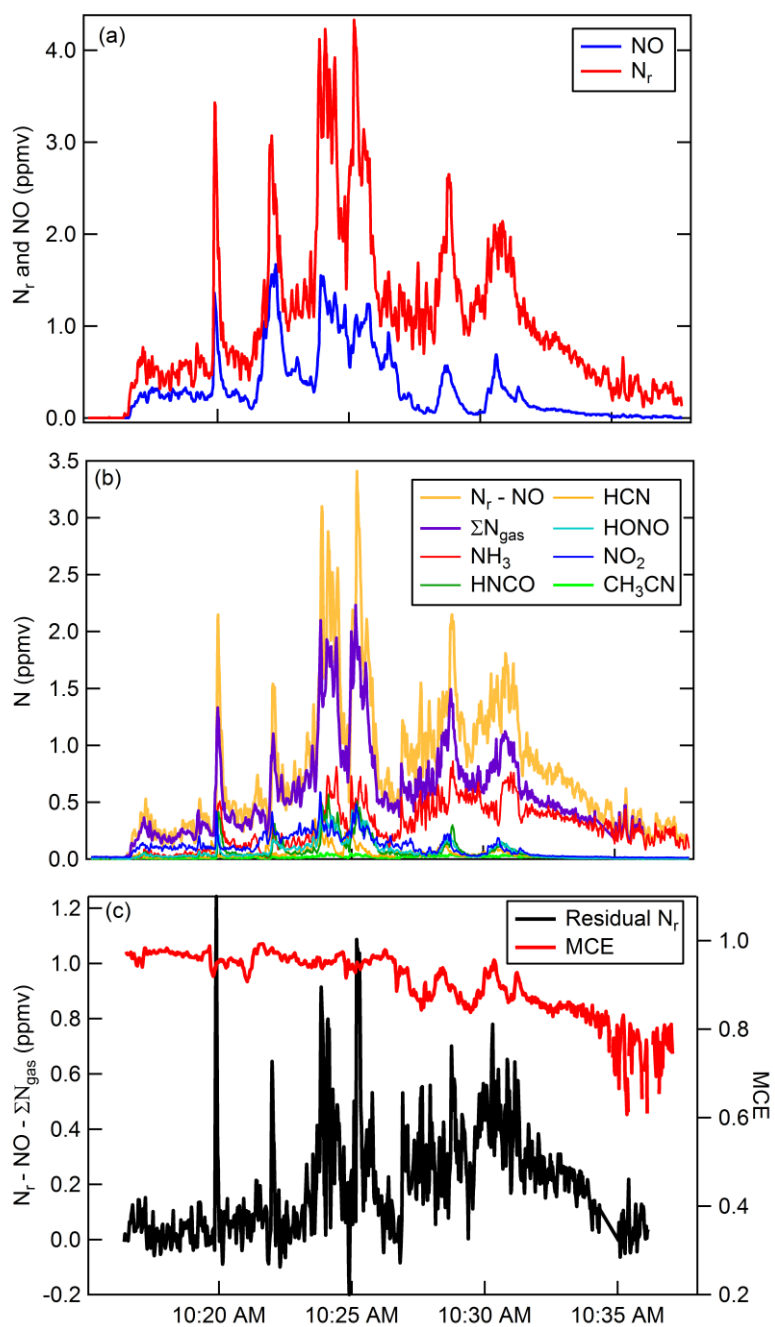
19 HNO₃ was not measured during the experiment though we'd expect very low concentrations from biomass burning as
20 much of the HNO₃ formed likely reacts quickly with NH₃ to form particle nitrate (Yokelson et al., 2009; see reference
21 below). The Reviewer brings up a useful suggestion to add MCE to the figure to better support the differences in
22 emissions between smoldering and flaming, therefore we have added MCE to panel (c) of Fig. 6 and the following
23 additions to the text:

24 See: Yokelson, R. J., Crounse, J. D., DeCarlo, P. F., Karl, T., Urbanski, S., Atlas, E., Campos, T., Shinozuka, Y.,
25 Kapustin, V., Clarke, A. D., Weinheimer, A., Knapp, D. J., Montzka, D. D., Holloway, J., Weibring, P., Flocke, F.,
26 Zheng, W., Toohey, D., Wennberg, P. O., Wiedinmyer, C., Mauldin, L., Fried, A., Richter, D., Walega, J., Jimenez,
27 J. L., Adachi, K., Buseck, P. R., Hall, S. R., and Shetter, R.: Emissions from biomass burning in the Yucatan, Atmos.
28 Chem. Phys., 9, 5785-5812, <https://doi.org/10.5194/acp-9-5785-2009>, 2009.

29 P11 L15 Added text: “The modified combustion efficiency (MCE) is a measure to estimate the relative contribution
30 of flaming and smoldering combustion that occurred over the course of a fire, where the MCE is defined as the ratio
31 of $\Delta\text{CO}_2 / (\Delta\text{CO}_2 + \Delta\text{CO})$ (Yokelson et al., 1996). A higher MCE value (approaching 0.99) designates relatively pure
32 flaming combustion (more complete oxidation) and a lower MCE (~ 0.75 – 0.84) designates more smoldering
33 combustion.”

34 P11 L16-17 Existing text: “it is likely that particulate ammonium contributes to the excess N_r signal measured during
35 periods dominated by smoldering combustion” New text: “it is possible that the residual signals are due to particulate
36 N-containing compounds. Particulate ammonium may contribute to the excess N_r signal measured during periods
37 dominated by smoldering combustion (MCE < 0.90).”

- 1 P11 L17-18 Existing text: “, while particulate nitrate likely accounts for some N_r signal during the flaming dominated
2 stages as shown in Fig. 6.” New text: “*The oxidized N-containing gas phase species are relatively more abundant*
3 *during the initial part of the fire, so particulate nitrate could account for some N_r signal during the flaming dominated*
4 *stages as shown in Fig. 6.*”
- 5 P32 Figure 6 caption; Existing text: “(c) Residual N_r in ppmv” New text: “(c) *Residual N_r (black) in ppmv with*
6 *modified combustion efficiency overlaid (MCE, red).*”
- 7 P25 L3 Add reference “Yokelson, R. J., Griffith, D. W. T., and Ward, D. E.: *Open path Fourier transform infrared*
8 *studies of large-scale laboratory biomass fires, J. Geophys. Res., 101, 21067–21080, doi:10.1029/96jd01800, 1996.*”
- 9 Please see updated Figure below:



1 7. typos: a. p.6, line 11: change "least-squared" to "least-squares" b. p. 6, line 35: change "promoted" to
2 "promote" p. 12, line 20: change "liens" to "lines"

3 Thank you for bringing these minor mistakes to our attention. We have corrected the mistakes as follows:

4 P6 L11 Existing text: "least-squared" New text: "least-squares"

5 P6 L35 Existing text: "promoted" New text: "promote"

6 P12 L20 Existing text: "liens" New text: "lines"

7 The following includes voluntary changes to references, which includes several updates

8 P21 L1-4 Update the Kupc reference to: "Kupc, A., Williamson, C., Wagner, N. L., Richardson, M., and Brock, C. A.:
9 Modification, calibration, and performance of the Ultra-High Sensitivity Aerosol Spectrometer for particle size
10 distribution and volatility measurements during the Atmospheric Tomography Mission (ATom) airborne campaign,
11 Atmos. Meas. Tech., 11, 369-383, <https://doi.org/10.5194/amt-11-369-2018>, 2018."

12 P7 L24 Change "Kupc et al. 2017" to Kupc et al., 2018"

13 P7 L31 Change "Kupc et al. 2017" to Kupc et al., 2018"

14 P7 L34 Change "Kupc et al. 2017" to Kupc et al., 2018"

15 P24 L9-11 Update the Selimovic reference to: "Selimovic, V., Yokelson, R. J., Warneke, C., Roberts, J. M., de Gouw,
16 J., Reardon, J., and Griffith, D. W. T.: Aerosol optical properties and trace gas emissions by PAX and OP-FTIR for
17 laboratory-simulated western US wildfires during FIREX, Atmos. Chem. Phys., 18, 2929-2948,
18 <https://doi.org/10.5194/acp-18-2929-2018>, 2018."

19 P11 L10 Change "Selimovic et al., 2017" to "Selimovic et al., 2018"

20 P20 L23-27 Update the Koss reference to: "Koss, A. R., Sekimoto, K., Gilman, J. B., Selimovic, V., Coggon, M. M.,
21 Zarzana, K. J., Yuan, B., Lerner, B. M., Brown, S. S., Jimenez, J. L., Krechmer, J., Roberts, J. M., Warneke, C.,
22 Yokelson, R. J., and de Gouw, J.: Non-methane organic gas emissions from biomass burning: identification,
23 quantification, and emission factors from PTR-ToF during the FIREX 2016 laboratory experiment, Atmos. Chem.
24 Phys., 18, 3299-3319, <https://doi.org/10.5194/acp-18-3299-2018>, 2018."

25 P11 L10 Change "Koss et al., 2017" to "Koss et al., 2018"

26

27

28

Characterization of a catalyst-based ~~total nitrogen and carbon~~ conversion technique to measure total particulate nitrogen and organic carbon and comparison to a calibrate particle mass measurement instrumentation

Chelsea E. Stockwell^{1,2}, Agnieszka Kupc^{1,2}, Bartłomiej Witkowski^{1,2,3}, Ranajit K. Talukdar^{1,2}, Yong Liu⁴, Vanessa Selimovic⁵, Kyle J. Zarzana^{1,2}, Kanako Sekimoto^{1,2}, Carsten Warneke^{1,2}, Rebecca A. Washenfelder¹, Robert J. Yokelson⁵, Ann M. Middlebrook¹, James M. Roberts¹

¹NOAA Earth System Research Laboratory (ESRL), Chemical Sciences Division, Boulder, CO 80305, USA

²Cooperative Institute for Research in Environmental Sciences, University of Colorado, Boulder, CO 80309, USA

³University of Warsaw, Faculty of Chemistry, al. Żwirki i Wigury 101, 02-089, Warsaw, Poland

⁴University of Colorado Denver, Department of Chemistry, Denver, CO 80217, USA

⁵University of Montana, Department of Chemistry, Missoula, MT 59812, USA

Correspondence to: C. E. Stockwell (Chelsea.Stockwell@noaa.gov); J. M. Roberts (James.M.Roberts@noaa.gov)

Abstract. The chemical composition of aerosol particles is a key aspect in determining their impact on the environment. For example, nitrogen (N)-containing particles impact atmospheric chemistry, air quality, and ecological N-deposition. Instruments that measure total reactive nitrogen (N_r = all nitrogen compounds except for N_2 and N_2O) focus on gas-phase nitrogen and very few studies directly discuss the instrument capacity to measure the mass of N_r -containing particles. Here, we investigate the mass quantification of particle-bound nitrogen using a custom N_r system that involves total conversion to nitric oxide (NO) across platinum and molybdenum catalysts followed by NO-O₃ chemiluminescence detection. We evaluate the particle conversion of the N_r instrument by comparing to mass derived concentrations of size-selected and counted ammonium sulfate ((NH₄)₂SO₄), ammonium nitrate (NH₄NO₃), ammonium chloride (NH₄Cl), sodium nitrate (NaNO₃), and ammonium oxalate ((NH₄)₂C₂O₄) particles determined using instruments that measure particle number and size. These measurements demonstrate N_r -particle conversion across the N_r catalysts that is independent of particle size with $98 \pm 10\%$ efficiency for 100 – 600 nm particle diameters. We also show efficient conversion of particle-phase organic carbon species to CO₂ across the instrument's platinum catalyst followed by a non-dispersive infrared (NDIR) CO₂ detector. However, the application of this method to the atmosphere presents a challenge due to the small signal above background at high ambient levels of common gas-phase carbon compounds (e.g. CO₂). We show the N_r system is an accurate particle mass measurement method and demonstrate its ability to calibrate particle mass measurement instrumentation using single component, laboratory generated, N_r -containing particles below 2.5 μ m in size. In addition we show agreement with mass measurements of an independently calibrated on-line particle-into-liquid sampler directly coupled to the electrospray ionization source of a quadrupole mass spectrometer (PILS-ESI/MS) sampling in the negative ion mode. We obtain excellent correlations ($R^2 = 0.99$) of particle mass measured as N_r with PILS-ESI/MS measurements converted to the

Formatted: Subscript

corresponding particle anion mass (e.g. nitrate, sulfate, and chloride). The N_r and PILS-ESI/MS are shown to agree to within ~6% for particle mass loadings up to $120 \mu\text{g m}^{-3}$. Consideration of all the sources of error in the PILS-ESI/MS technique yields an overall uncertainty of $\pm 20\%$ for these single component particle streams. These results demonstrate the N_r system is a reliable direct particle mass measurement technique that differs from other particle instrument calibration techniques that rely on knowledge of particle size, shape, density, and refractive index.

1 Introduction

Aerosol particles are a key component of the atmospheric chemical environment as they have climate, human health, and ecosystem effects (Pöschl, 2005; IPCC, 2013). Measuring aerosol particle chemical composition is a challenging endeavor that has been the subject of a great deal of innovation in the past few decades (Jayne et al., 2000; Weber et al., 2001; Jimenez et al., 2009; Hallquist et al., 2010). The calibration of these instruments has evolved to better detect speciated composition. Still, there is a need for fundamental mass-based calibration techniques to place aerosol particle measurements firmly in the context of other atmospheric chemical observations.

Nitrogen (N) compounds are major constituents of atmospheric aerosol and play a significant role in atmospheric chemistry, radiative balance, air quality, and N-deposition in both terrestrial and aquatic ecosystems (Neff et al., 2002; Liao et al., 2003; Forster et al., 2007; Cornell, 2010; Xu et al., 2012; Park et al., 2014; Fuzzi et al., 2015). The relative contribution of N-compounds, specifically particulate nitrate, to total atmospheric particle mass is expected to increase in the coming century due to a projected reduction in SO_2 and increasing NH_3 (Bauer et al., 2007; Bellouin et al., 2011; Hauglustaine et al., 2014; Li et al., 2015), and already dominates in some urban and agricultural environments (Haywood et al., 2008; Vieno et al., 2016). Excluding N-species in deposition studies contributes to uncertainty in regional and global nitrogen budgets used to evaluate ecological, biogeochemical, and climate impacts (Jickells et al., 2013; Cornell, 2010; Cape et al., 2011). Measuring individual N-species, classes of N-compounds, or total N is challenging, and laboratory and field data are limited. For example, while there are a number of methods to measure inorganic N species, particulate organic N is more difficult to quantify with fewer sampling and measurement methods currently available for such a variety of compounds (Lin et al., 2010; Farmer et al., 2010; Lee et al., 2016). Measuring the total N mass of atmospheric particles will improve our understanding of their role in nitrogen cycles associated with sources such as agriculture or wildfires, and processes such as photochemical oxidation.

Several techniques exist to measure total reactive nitrogen (N_r), defined here as all atmospheric nitrogen excluding N_2 and N_2O , which includes both gas (e.g. total odd nitrogen (NO_y), NH_3 , amines, nitriles, nitrates, etc.) and particle phase species (e.g. inorganic and organic N compounds). An established, rapid-response, robust technique for measuring N_r involves thermal and catalytic conversion to nitric oxide (NO) with detection by [ozone \(\$\text{O}_3\$ \)](#) chemiluminescence. The catalyst material, temperature, and sampling methods dictate the efficiency, time resolution, and speciation of measurements (Winer et al., 1974; Williams et al., 1998; Dunlea et al., 2007; Schwab et al., 2007; Benedict et al., 2017). The chemiluminescence detection technique has been used to measure NO_x ($\text{NO} + \text{NO}_2$; Parrish and Fehsenfeld, 2000), total gas-phase N_r (e.g. Hardy and Knarr, 1982; Horstman, 1982), individual reactive nitrogen components (e.g. NH_3 ; Breitenbach and Shelef, 1973; Saylor et al., 2010), or subsets of nitrogen compounds by removal of selected compounds using filters or denuders upstream (Prenni et al., 2014). Marx et al. (2012) completed

the only study to explicitly report quantitative conversion of particle-bound N_r for a limited number of species, however the results show a range of conversion efficiencies (78 – 142%). Several other studies assume at least some (non-quantitative) particle conversion across their catalysts (Fahey et al., 1985, 1986; Prenni et al., 2014). To our knowledge, no study selectively isolates particle-phase reactive nitrogen to assess the particle-phase contribution to total nitrogen signals from individual sources or in their atmospheric measurement. Here we characterize the particulate N_r conversion in our converter consisting of heated platinum and molybdenum catalysts followed by rapid chemiluminescence detection using common inorganic atmospheric N_r -species including $(NH_4)_2SO_4$, NH_4Cl , $NaNO_3$, NH_4NO_3 , and $(NH_4)_2C_2O_4$. The application of the converter coupled with $NO-O_3$ chemiluminescence, hereafter referred to as the N_r system, to quantitatively convert and measure the sum of N_r particle mass was evaluated using mass concentrations determined using traditional particle instrument calibration methods.

Organic carbon species are major constituents of aerosol particles (Jimenez et al., 2009) and are responsible for some of the more important climate and health impacts of particles (Pöschl, 2005). Calibration of measurement systems for organic carbon species is a challenging task since there are thousands of possible compounds of differing sizes, functional groups and therefore volatilities (Jimenez et al., 2016; Murphy, 2016a, b). A comprehensive, mass-based technique for organic aerosol species would be a highly-desirable addition to the current measurement technology. Theoretically, the high-temperature platinum catalyst in our system should convert carbon species to carbon-dioxide (CO_2) in the presence of air. Conversion of volatile organic compounds (VOCs) to CO_2 on high temperature precious metal catalysts is a well-developed technique (see for example the Pt catalyst used in Veres et al., 2010). Total organic carbon measurements using similar catalysts (e.g. palladium/alumina) followed by reduction to methane have been used previously (Roberts et al., 1998; Maris et al., 2003). ~~By these methods, Roberts et al. (1998) confirmed efficient conversion of C_4 - C_2 gas-phase compounds across the catalyst.~~ Platinum-based catalysts are widely used and have been shown to be more efficient than palladium in oxidation studies (Schwartz et al., 1971; Kamal et al., 2016). Here we characterize the conversion efficiency of particle-phase organic carbon across our Pt catalyst by direct measurements using a LICOR non-dispersive infrared (NDIR) CO_2 analyzer. The current converter ~~specifications design~~ coupled with both NO and CO_2 detectors allows simultaneous measurements of N_r and total carbon (C_T).

Many traditional particle instrument calibration methods involve measurements of particle properties by inertial, gravitational, diffusional, electrical (e.g. sizing), thermal, or optical measurement devices (Chen et al., 2011). Generally, direct mass concentration calibration techniques involve off-line analysis of filters or semi-real time measurements (e.g. PILS combined with ion chromatography). More rapid techniques directly measure number concentrations and particle sizes. However, these methods often require knowledge of aerosol properties (e.g. composition, shape, density, refractive index) and sampling parameters (e.g. volumetric flow rate, pressure, temperature, relative humidity) in order to determine mass concentrations. ~~While these instrument calibration techniques are well-established for controlled laboratory-generated aerosol standards,~~ The N_r system is an alternative that directly measures mass traced back to gas phase calibration standards instead of relying on particle size, shape, or refractive index.

In order to demonstrate the application of the N_r system to directly measure particle mass to calibrate particle mass measurement instrumentation, we compare mass concentrations measured by a new approach of directly coupling a particle-into-liquid sampler to the electrospray ionization source of a quadrupole mass spectrometer (PILS-ESI/MS) for on-line mass analysis of water-soluble aerosols. The Particle-into-Liquid Sampler (PILS) is an established technique developed to efficiently collect the water-soluble fraction of aerosol (Weber et al. 2001; Orsini et al., 2003; Sorooshian et al., 2006). Here, we couple the PILS with an independently calibrated electrospray interface followed by mass spectrometric detection to obtain on-line mass measurements of single-component, laboratory generated, N_r -containing aerosol that can be directly calibrated using the N_r system.

In this work, we present the converter set-up, system methodology, and evaluate the particle-conversion efficiency of a custom N_r system for several atmospherically relevant N_r -containing particles. The conversion efficiency of the N_r -catalyst was evaluated by comparing the N_r mass signal with the mass calculated from instrument calibration techniques that measure the particle number size distributions of laboratory-generated aerosols of known composition. We then show the quantitative conversion of organic carbon across the instrument's platinum catalyst followed by CO_2 detection. Finally we compare particle mass directly measured using a particle-into-liquid sampler coupled directly to an electrospray ionization source and the PILS-ESI/MS with that measured by the N_r instrument. The primary objectives of these experiments is to characterize particle conversion in the N_r system, and to investigate the capabilities of the N_r system as a calibration instrument that directly measures particle mass concentration.

2 Experimental details

2.1 Instrument descriptions

2.1.1 Description of the total-Total reactive nitrogen (N_r) system

Measurements of total reactive nitrogen, N_r , were accomplished by catalytic conversion to NO and detection of the NO using a chemiluminescence instrument. This NO- O_3 chemiluminescence instrument is a custom-built version of the common atmospheric monitoring instrument (Williams et al., 1998) and is calibrated directly with gas phase standards of NO. All the N_r species were converted to NO or NO_2 on a high temperature catalyst, and the NO_2 subsequently converted to NO on a lower temperature catalyst. The high-temperature catalyst system consisted of a quartz tube (13 mm OD x 11 mm ID x 35 cm L) packed with 36 platinum (Pt) screens (Shimadzu Part No. 630-00105) run at high temperature (750°C), shown in Fig. 1. The catalyst bed was confined to an 8 cm long section by dimples in the quartz tube, and that section was positioned so that the gas reaching it had been equilibrated to 750°C, as confirmed by a thermocouple probe. The flow through the catalyst was set to 1 standard L min^{-1} via a downstream flow controller. The Pt surface area was 126 cm^2 and the residence time was 0.1 s at 83.3 kPa and 750°C. Platinum catalysts of this kind are also known to oxidize NO to NO_2 , which has been the source of problems with some previous systems that were designed to measure atmospheric ammonia (NH_3) (Schwab et al., 2007). In our system, the Pt catalyst is followed by a molybdenum oxide (MoOx) catalyst consisting of a solid molybdenum tube (4.2 mm ID x 32 cm L) operated at 450°C, to which an 8 standard $cm^3 min^{-1}$ flow of pure hydrogen was added to create a stable

Formatted: Line spacing: single

Formatted: Font: Bold

molybdenum oxide surface. Run in this manner, the MoO_x surface did not require periodic treatment at higher temperatures under reducing conditions as described by Williams et al. (1998). The heated MoO_x catalyst reduces the remaining NO₂ to NO. The NO chemiluminescence detection scheme used for laboratory calibrations had a fundamental sensitivity between 6 and 7 counts per parts per trillion (pptv) and the detection limit determined by the background signal in zero air was typically 0.15 pptv (4 σ) for a 1 s measurement. The operation of this instrument during these experiments often required considerable de-tuning to keep the instrument count rates below the roll-over point of the photon counting electronics (approximately 5 MHz) for the particle concentrations generated, thus the detection limit was closer to 0.1 ppbv (corresponding to 0.3 $\mu\text{g m}^{-3}$ for aerosol nitrate) for these measurements.

Formatted: Subscript

Formatted: Font: Not Italic

2.1.2 Total carbon (C_T) system

Formatted: Subscript

Formatted: Heading 2, Left, Indent: First line: 0", Line spacing: single

Measurements of total carbon (C_T) were accomplished by catalytic conversion to carbon dioxide (CO₂) and detection using a CO₂ analyzer. The high-temperature (750°C), platinum catalyst (Fig. 1) in the N₂ system should quantitatively convert carbon containing species to CO₂ in the presence of air. Gas-phase carbon conversion across similar precious metals has been studied extensively (see for example the Pt catalyst used in Veres et al., 2010). The total flow through the Pt catalyst was set to ~1.5 standard L min⁻¹ and was then split before the MoO_x catalyst. In our sampling scheme 0.5 sL min⁻¹ of flow was directed to a LICOR 6251 (LI-6251; Lincoln, NE) CO₂ analyzer, while the remaining flow, 1 sL min⁻¹, was directed through the MoO_x catalyst and to the NO-O₃ chemiluminescence detector as detailed in Sect. 2.1.1. Run in this manner, the conversion of compounds that contain both N and C atoms can then be measured simultaneously using the NO-O₃ chemiluminescence detector and LI-6251 detector in parallel. The LICOR instrument was internally referenced to scrubbed zero air. At ambient CO₂ levels, it is challenging to retrieve reliable measurements since the signal relative to the background abundance of CO₂ is small. In order to evaluate organic carbon conversion efficiency, our approach relies on using ultra-pure air for aerosol generation and carrier gas flow, therefore ambient CO and CO₂ is eliminated. The LI-6251 was calibrated with sub-5 ppm CO₂ standards (Scott-Marín Inc., Riverside, CA) in ultra-pure air. Due to the low signals levels and the uncertainty of the low concentration CO₂ standards, the overall uncertainty of the CO₂ measurements below 1 ppmv presented in this work is $\pm 10\%$ for 10 second averages.

Formatted: Left, Indent: First line: 0", Line spacing: Multiple 1.15 li

2.1.3 PILS-ESI/MS

Formatted: English (United Kingdom)

A schematic of the PILS-ESI/MS is shown in Fig. 2. The Particle-into-Liquid Sampler (PILS; Brechtel Manufacturing Inc., Hayward, CA) was developed by Weber et al. (2001) and collects water-soluble aerosol compounds by growing particles into liquid droplets in a supersaturated water environment and then collecting the droplets. A detailed description of the PILS can be found in Sorooshian et al. (2006). The PILS is an established water-soluble aerosol collection technique that has been coupled with various mass analysis methods and was used previously by other laboratories in instrument evaluation studies (e.g. Drewnick et al., 2003; Takegawa et al., 2005; Canagaratna et al., 2007).

The PILS liquid outlet flow was set to 100 $\mu\text{L min}^{-1}$ and was continuously mixed with an acetonitrile flow (100 $\mu\text{L min}^{-1}$). The 1:1 volume mixture of acetonitrile and water was directed toward the custom electrospray ionization source (at ~10 $\mu\text{L min}^{-1}$) of a commercial quadrupole mass spectrometer (Balzers Instruments, QMG 422) operated in negative ion mode for on-line analysis of selected water-soluble organic and inorganic compounds. The

electrospray interface involved sample injection at ambient pressure through a fused silica capillary tip (30 μ M ID) with a 2.5 L min⁻¹ N₂ sheath flow at a spray voltage of -3.5 kV. The MS instrument was modified from the negative-ion proton-transfer chemical-ionization mass spectrometer (NI-PT-CIMS) described in Veres et al. (2008). The flow tube was replaced with a stainless steel capillary inlet connected to the front region (I; shown in Fig. 2) held at ~300 Pa. Ions were focused across this region using a planar DC ion carpet (Anthony et al., 2014) mounted in front of the orifice leading to the second region (II). The ions were then accelerated through the collisional dissociation chamber (CDC) and collimated in the octopole ion guide at a total pressure of ~1 Pa (region II). The ions were transferred to the quadrupole mass spectrometer (region III). The electron multiplier detector was maintained at a pressure of less than 6.6×10^{-3} Pa.

The ESI/MS was calibrated using volumetrically and gravimetrically prepared liquid-phase standards of the anions associated with the target compounds (e.g. SO₄²⁻, NO₃⁻, Cl⁻) (Sigma Aldrich, St. Louis, MO). Anion-specific calibration factors were calculated from linear least-squares fits of multi-point calibration curves. The uncertainty in the slope resulted in a maximum uncertainty of ~10% for the compounds tested. The ESI flow rate, solvent composition, analyte chemical properties, and matrix effects potentially impact the ionization and transmission efficiencies of compounds (Kostiainen and Kauppinen, 2009). For these reasons, experiments were performed under similar, or as close to identical, conditions as the calibrations for instrument evaluation. The limits of detection for the anions measured with the PILS-ESI/MS were below ~0.1 μ g m⁻³ for the current system and sampling conditions. Sorooshian et al. (2006) discuss volatility losses in the PILS for several inorganic species and reported negligible loss with a collection efficiency of $\geq 96\%$ for mass loadings of Cl⁻, SO₄²⁻, and NO₃⁻ ranging from 1-140 μ g m⁻³. Additionally, Orsini et al. (2003) showed the collection efficiency of $\geq 95\%$ for particles as small as 30 nm diameter for a 15 L min⁻¹ sample flow rate. Ammonium (NH₄⁺) is the major ion susceptible to volatilization as shown in Ma (2004), who indicated an underestimation of ~15%. In this study, because we were operating in the negative-ion mode, we did not measure NH₄⁺ directly.

2.2 Experimental design

2.2.1 Methods for determining gas-phase conversion efficiency

The efficiency of conversion of several N-containing gases by the N_r catalyst was determined through addition of a number of representative compounds that were calibrated independently. The NO signal from the converted species was then compared to the signal from an NO in N₂ standard (5.38 ppmv, Scott-Marrin Inc., Riverside, CA) that was used as the working standard for this project. Typical calibration levels were in the range of 50 to 100 ppbv as determined by the mass flow controllers used to mix the standard into the measurement stream. The standards used for each compound and their associated calibrations were as follows.

The NO₂ standard stream was produced from the NO working standard through gas-phase titration with a small stream of O₂ in which O₃ had been produced by photolysis at 184.9 nm using a mercury discharge lamp. This technique is used routinely for NO_x and NO_y measurement systems (Williams et al., 1998) and allows straightforward determination of NO₂ conversion provided care is taken not to over-titrate the NO stream to produce NO₃ and therefore

1 N₂O₅. The uncertainty in the NO₂ conversion determination is simply the propagated errors in the subtraction of the
2 signals before and after titration.

3 The ammonia (NH₃) conversion was examined using two different NH₃ sources, a gas mixture (3.1 ppmv in
4 N₂, Scott-Marrin) and a permeation device (Kin-Tek, LaMarque, Texas). Care was taken with these standards to keep
5 them under flow for periods of several days in order to insure any system surfaces were equilibrated. The calibration
6 of these standards was accomplished by ultraviolet (UV) absorption spectroscopy at 184.9 nm wavelength using an
7 instrument described by Neuman et al, (2003), and based on absorption cross-sections reported in the literature
8 (Tannenbaum et al., 1953; Lovejoy, 1999; Froyd, 2002). The uncertainty of NH₃ conversion was propagated based on
9 the uncertainties in flow rate and UV absorption determinations.

10 The hydrogen cyanide (HCN) standard consisted of a commercial gravimetric mixture of HCN in N₂ (10
11 ppmv GASCO Oldsmar, FL), which was mixed into the system using a mass flow controller. The specified uncertainty
12 of this mixture was ±10%, and the standard concentration was verified using long-path Fourier-transform infrared
13 (FTIR) spectroscopy to within the stated uncertainty. The HCN standard was used to produce a gas phase stream of
14 cyanogen chlorine (ClCN) by reaction with chloramine-T, a non-volatile chlorinating agent, which has been described
15 previously (Valentour et al., 1974). To do this, a small stream (5 standard cm³ min⁻¹) of the HCN standard was
16 combined with humidified Zero Air (ZA, 60% RH, 30 standard cm³ min⁻¹) over a bed packed with glass beads coated
17 with a solution of chloramine-T. The glass beads were prepared by coating glass 3 mm outer diameter (OD) beads
18 with a 2 g 100 mL⁻¹ solution and packing ~20 cm³ of them in a 12.7 mm OD PFA tube and flowing ZA over them
19 until dry. The reaction was shown to be essentially 100% (±10%) by proton-transfer reaction mass spectrometry (PTR-
20 MS) when conducted in a humidified atmosphere (RH ≥60%), by FTIR analysis of the HCN and ClCN in the gas
21 stream before and after chlorination.

22 The isocyanic acid (HNCO) standard was prepared according to the methods described by Roberts et al.
23 (2010), in which the trimer, cyanuric acid, was thermally decomposed at 250°C in a diffusion cell to produce a steady
24 stream of HNCO, which was then calibrated by long-path FTIR spectroscopy. Initially, this source has the potential
25 to produce NH₃ as an impurity, most likely because of the presence of trace amounts of water. Keeping the source
26 under flow and above 120°C at all times when not in use was found to reduce the NH₃ impurity to negligible levels
27 (<5%), as measured by PTR-MS. The uncertainties in the HNCO standard were propagated from the uncertainties in
28 the HNCO cross section (Northwest-Infrared, PNNL), the NH₃ subtraction, and flow rates. Standard streams of both
29 nitrobenzene and trimethylamine were produced using gravimetrically prepared solutions and a commercial liquid
30 calibration device (Ionicon, Innsbruck, Austria). The uncertainties in these liquid calibration standards were estimated
31 from the propagated uncertainties in the solution concentrations and the liquid and gas flow rates.

32 The conversion of nitrous oxide (N₂O) is a potential interference in the N_x method as N₂O is not typically
33 considered a reactive nitrogen compound in the troposphere. Several experiments were conducted to determine the
34 extent of this potential interference using a 10.1 ppmv N₂O standard. The resulting conversion efficiency ranged from
35 0.03% to 0.05% in dry and humidified air respectively. These can be considered upper limits for this interference as
36 we cannot be completely sure that there were no N_x contaminants (e.g. NO₂) in the N₂O standard.

2.1.1 Nitrogen-containing particles

The measurement of particle-phase N_r requires decomposition or volatilization of the solid material, followed by catalytic conversion to NO (or NO_2). Broadly, there are three types of N_r -containing particles, with a range of thermal stabilities from volatile to refractory. First, there is considerable literature that indicates that small particles composed of two major semi-volatile species, ammonium nitrate (NH_4NO_3) and ammonium chloride (NH_4Cl), will dissociate to constituents NH_3 and HNO_3 (and HCl), when modestly heated to temperatures $< 100^\circ C$ (Huffman et al., 2009; Hu et al., 2011). These materials will be readily converted on high-temperature catalysts (e.g. platinum, Pt) as gas-phase NH_3 and HNO_3 . The second type of N_r -containing particles include intermediate stability compounds consisting mostly of nitro-organics ($R-NO_2$), organic nitrates ($RONO_2$), and amine and ammonium salts of acids. These compounds begin to decompose at relatively low temperatures. For example, thermal decomposition studies of bulk ammonium oxalate ($(NH_4)_2C_2O_4$) indicate that it begins to decompose at temperatures slightly above $200^\circ C$ (Usherenko et al., 1998). Similarly, bulk samples of ammonium sulfate ($(NH_4)_2SO_4$) and ammonium bisulfate ($(NH_4)HSO_4$) decompose at approximately 150 – $250^\circ C$ depending on water content (Kiyoura and Urano, 1970). Given sufficient residence time, intermediate volatility compounds will start to convert to gas-phase products in the hot inlet tubing and fully convert to NO (or NO_2) on a hot Pt surface ($750^\circ C$). The third type of N_r -containing particles are composed of refractory salts such as sodium nitrate ($NaNO_3$), which will be the most resistant to decomposition and require contact with high-temperature surfaces of the Pt catalyst. Studies of the thermal decomposition of $NaNO_3$ on Pt surfaces indicate that NO is evolved starting at about $500^\circ C$. In summary, the existing literature suggests that the thermal decomposition/conversion of N_r -containing particles to NO (NO_2) is thermodynamically feasible provided there is sufficient residence time and surface area in the catalyst zone.

2.2 Description of the PILS-ESI/MS

A schematic of the PILS-ESI/MS is shown in Fig. 2. The Particle-into-Liquid Sampler (PILS; Brechtel Manufacturing Inc., Hayward, CA) was developed by Weber et al. (2001) and collects water-soluble aerosol compounds by growing particles into liquid droplets in a supersaturated water environment and then collecting the droplets. A detailed description of the PILS used in these studies can be found in Sorooshian et al. (2006). The PILS is an established water-soluble aerosol collection technique that has been coupled with various mass analysis methods and was used previously by other laboratories in instrument evaluation studies (e.g. Drewnick et al., 2003; Takegawa et al., 2005; Canagaratna et al., 2007).

The PILS sample flow was set to $100 \mu L \min^{-1}$ and was continuously mixed with an acetonitrile flow ($100 \mu L \min^{-1}$). The 1:1 volume mixture of acetonitrile and water was directed toward the custom electrospray ionization source (at $\sim 10 \mu L \min^{-1}$) of a commercial quadrupole mass spectrometer (Balzers Instruments, QMG 422) operated in negative ion mode for on-line analysis of selected water-soluble organic and inorganic compounds. The electrospray interface involved sample injection at ambient pressure through a fused-silica capillary tip ($30 \mu M$ ID) with a $2.5 L \min^{-1} N_2$ sheath flow at a spray voltage of ~ 3.5 kV. The MS instrument was modified from the negative ion proton-transfer chemical ionization mass spectrometer (NI-PT-CIMS) described in Veres et al. (2008). The flow tube was replaced with a stainless steel capillary inlet connected to the front region (I; shown in Fig. 2) held at ~ 300 Pa. Ions

were focused across this region using a planar DC ion carpet (Anthony et al., 2014) mounted in front of the orifice leading to the second region (II). The ions were then accelerated through the collisional dissociation chamber (CDC) and collimated in the octopole ion guide at a total pressure of ~ 1 Pa (region II). The ions were transferred to the quadrupole mass spectrometer (region III). The electron multiplier detector was maintained at a pressure of less than 6.6×10^{-3} Pa.

The ESI/MS was calibrated using volumetrically and gravimetrically prepared liquid-phase standards of the anions associated with the target compounds (e.g. SO_4^{2-} , NO_3^- , Cl^-) (Sigma Aldrich, St. Louis, MO). Anion-specific calibration factors were calculated from linear least-squared fits of multi-point calibration curves. The uncertainty in the slope resulted in a maximum uncertainty of $\sim 10\%$ for the compounds tested. The ESI flow rate, solvent composition, analyte chemical properties, and matrix effects potentially impact the ionization and transmission efficiencies of compounds (Kostiainen and Kauppinen, 2009). For these reasons, experiments were performed under similar, or as close to identical, conditions as the calibrations for instrument evaluation. For purposes of this comparison, matrix effects were assumed to be negligible for tests sampling single-component aerosols. The limits of detection for the anions measured with the PILS-ESI/MS were below $\sim 0.1 \mu\text{g m}^{-3}$ for the current system and sampling conditions. Sorooshian et al. (2006) discuss volatility losses in the PILS for several inorganic species and reported negligible loss with a collection efficiency of $\geq 96\%$ for mass loadings of Cl^- , SO_4^{2-} , and NO_3^- ranging from 1 – $140 \mu\text{g m}^{-3}$. Additionally, Orsini et al. (2003) showed the collection efficiency of $\geq 95\%$ for particles as small as 30 nm diameter for a 15 L min^{-1} sample flow rate. Ammonium (NH_4^+) is the major ion susceptible to volatilization as shown in Ma (2004), who indicated an underestimation of $\sim 15\%$. In this study, because we were operating in the negative-ion mode, we did not measure NH_4^+ directly.

2.3–2.2 Particle-generation, measurement, and characterization Methods for determining particle phase conversion efficiency

Several aerosols were generated including polystyrene latex spheres (PSL; Nanosphere size standards, Thermo Fisher Scientific Inc., Waltham, MA), NH_4NO_3 , $(\text{NH}_4)_2\text{SO}_4$, $(\text{NH}_4)_2\text{C}_2\text{O}_4$ (Sigma Aldrich, St. Louis, MO), NH_4Cl (J.T. Baker Chemical Co., Phillipsburg, NJ), and NaNO_3 (Fisher Scientific, Hampton, NH). Aerosol particles were generated by atomization-atomizing of aqueous solutions of pure compounds in distilled water (~ 0.5 – 6 g L^{-1}) using a custom-built Collison-type atomizer (similar to one reported by Liu and Lee, 1975) in a dry particle-free nitrogen or zero air flow. The output flow was dried using a silica gel diffusion dryer to a relative humidity less than 10% . The dry polydisperse particles were then size-selected using a custom-built differential mobility analyzer (DMA; similar to one described by Knutson and Whitby, 1975). The DMA was operated at a sample flow of 0.3 – 0.5 volumetric L min^{-1} and a ratio of $10:1$ between the sheath and sample flow. The monodisperse particles were diluted with ultra-high purity filtered zero air (range 1 – 10 L min^{-1}) before entering a mixing vessel. In instances where a mixing vessel was not available, a segment of smaller diameter tubing was added in-line to promote mixing prior to the flow being divided among the instruments. A condensation particle counter (CPC; 3022A, TSI Inc., Shoreview, MN) (Stolzenburg and McMurry, 1991) continuously measured the particle number concentration of the DMA output flow, following dilution. We measured the CPC flow rate pre- and post-sampling using a low-flow DryCal (Mesa

Laboratories, Lakewood, CO) and estimate an uncertainty in the CPC flow rate calibration to be $\pm 1\%$. During several experiments, the aerosol flow was split and sampled by an ultra-high sensitivity aerosol spectrometer (UHSAS; Droplet Measurement Technologies, Longmont, CO) to continuously measure the particle concentration and size distribution for particles with diameters between ~ 63 and 1000 nm.

In these experiments particle diameters from 100 to 600 nm were selected and the multiply-charged particles in the size distribution were accounted for as described below. For the liquid concentrations and atomizer conditions we used, For the liquid concentrations, atomizer conditions, and DMA settings used here, the DMA output size distribution is was a multi-peaked population consisting not only of singly charged particles but also particles with multiple (mostly two or three) charges that. The multiply-charged particles can contribute significantly to the overall mass and must be considered when calculating particle mass. The distributions of singly, doubly, and triply charged particles can vary depending on the solution concentration. Hence the particle mass could not be calculated directly from the singly-charged mobility diameter, particle density, and the CPC number concentrations. We generally used two methods to calculate the particle mass concentrations for these experiments. For the first method, the size distributions were measured using We measured atomized size distributions using the scanning mobility particle sizer (SMPS; Wang and Flagan, 1990) function of the DMA (physical diameter, $D_p = 1$ - 1000 nm). We used the DMA transfer theory (Knutson and Whitby, 1975; Stolzenburg, 1988) with Wiedensohler's (1988) steady-state charge distribution approximation was used to estimate the fraction of multiply charged particles contributing to the CPC number concentration for each diameter setting. There are a number of possible sources of uncertainty using these methods that may include particle losses, DMA transfer function uncertainty, counting uncertainty, and inversion errors. When comparing mass concentrations from the SMPS with those measured by the Nr system, issues with the SMPS-derived size distributions became apparent (discussed separately in Section 3.2.2). For the second method of calculating mass concentrations, we directly measured the diluted, DMA output. Consequently, the size distribution of particles selected at a particular voltage and flow setting of the DMA was examined using the UHSAS. UHSAS particle sizing is a function of the amount of light scattered onto the photodetectors, which. The quantity of scattered light, however, depends not only on the particle size, but also on the composition-dependent particle refractive index (Bohren and Huffman, 1983; Liu and Daum, 2000; Hand and Kreidenweis 2002; Rosenberg et al., 2012). The UHSAS manufacturer recommended calibration uses PSL microspheres, which are well characterized and have known refractive index ($n = 1.58$) and shape. Because the UHSAS sizing is sensitive to particle refractive index, a new sizing calibration curve was produced for each studied particle type (i.e. refractive index) using a DMA to select particles for a range of known sizes (Kupc et al., 20172018). Considering this, we used the DMA, with sizing accuracy $\pm 2.5\%$ and NIST traceable PSLs for 150 – 500 nm spheres as our calibration standard. The UHSAS sizing was recalibrated by using the DMA to select particles of known size for each of the aerosol types studied. A different UHSAS calibration curve was produced and used for each aerosol type (e.g. Kupe et al., 2017). These calibration curves were used to retrieve accurate particle size distributions so that properly accounted for the multiply charged particles, were properly accounted for.

Differences in particle counting efficiency between the UHSAS and CPC are potentially important. Previous laboratory studies show UHSAS and CPC number concentration comparisons in excellent agreement (Cai et al., 2008;

Kupc et al., 2017, 2018), however, occasionally only a ~90% counting efficiency for the UHSAS was observed when compared to the CPC. These differences are attributed to particle coincidence at high concentrations ($> 1000 \text{ cm}^{-3}$), and to inefficient particle mixing before reaching the instruments. Corrections for particle coincidence were applied (Kupc et al., 2017, 2018) though we expect differences due to particle mixing adds an additional 10% uncertainty to the measurements. For these reasons, we used the UHSAS size distributions to estimate the fraction of singly, doubly, and triply charged particles together with the total particle number taken from the CPC measurement to exclusive particle mass from total volume and density. The UHSAS and CPC measured particle number concentrations were generally within 10% of each other, however, the CPC values did not require coincidence corrections and had a better signal to noise ratio. Due to problems with measuring SMPS size distributions and requiring coincidence corrections for the UHSAS number concentrations, we used the UHSAS size distributions with the total particle number taken from the CPC measurement to calculate particle mass from total volume and density.

2.2.2 Nitrogen-containing particles

The measurement of particle phase N_r requires decomposition or volatilization of the solid material, followed by catalytic conversion to NO (or NO_2). Broadly, there are three types of N_r -containing particles, with a range of thermal stabilities from volatile to refractory. First, there is considerable literature that indicates that small particles composed of two major semi-volatile species, ammonium nitrate (NH_4NO_3) and ammonium chloride (NH_4Cl), will dissociate to constituents NH_3 and HNO_3 (and HCl), when modestly heated to temperatures $< 100^\circ\text{C}$ (Huffman et al., 2009; Hu et al., 2011). These materials will be readily converted on high temperature catalysts (e.g. platinum, Pt) as gas phase NH_3 and HNO_3 . The second type of N_r -containing particles include intermediate stability compounds consisting mostly of nitro-organics (R-NO_2), organic nitrates (RONO_2), and amine and ammonium salts of acids. These compounds begin to decompose at relatively low temperatures. For example, thermal decomposition studies of bulk ammonium oxalate ($(\text{NH}_4)_2\text{C}_2\text{O}_4$) indicate that it begins to decompose at temperatures slightly above 200°C (Usherenko et al., 1998). Similarly, bulk samples of ammonium sulfate ($(\text{NH}_4)_2\text{SO}_4$) and ammonium bisulfate ($(\text{NH}_4)\text{HSO}_4$) decompose at approximately $150\text{--}250^\circ\text{C}$ depending on water content (Kiyoura and Urano, 1970). Given sufficient residence time, intermediate volatility compounds will start to convert to gas-phase products in the hot inlet tubing and fully convert to NO (or NO_2) on a hot Pt surface (750°C). The third type of N_r -containing particles are composed of refractory salts such as sodium nitrate (NaNO_3), which will be the most resistant to decomposition and require contact with high temperature surfaces of the Pt catalyst. Studies of the thermal decomposition of NaNO_3 on Pt surfaces indicate that NO is evolved starting at about 500°C . In summary, the existing literature suggests that the thermal decomposition/conversion of N_r -containing particles to NO (NO_2) is thermodynamically feasible provided there is sufficient residence time and surface area in the catalyst zone.

3 Results and discussionInstrument characterization

3.1 Characterization of the N_r system

3.1.1 N_r gas-phase conversion efficiency

We verified the efficiency of conversion of a range of gas phase N_r compounds in this catalyst system using calibrated gas mixtures or standard streams and auxiliary analysis methods as described in Sect. 2.2.1. We compared the total N_r signal measured as NO_x, where NO_x was calibrated using NO standards in nitrogen (Scott-Marrin Inc., Riverside, CA) to the known amount specified by the calibration method. The conversion efficiencies are summarized in Table 1 and range from 95% to 110%. The values were based on the ratios of the N_r measured as NO to the expected values specified by each calibration method. The uncertainties in the measured conversion efficiencies encompass are in the propagated errors in each calibration method, and in all cases the range encompasses 100% conversion. For example, the largest uncertainty in the NH₃ conversion efficiency was the NH₃ UV absorption cross section at 184.9 nm (value of $4.4 \pm 0.3 \times 10^{-18}$ cm² taken from Neuman et al., 2003). It is possible that there were N_r compounds in the standard stream aside from NH₃ that were responsible for the result being >100%. However, the fact that the determination was above 100% for both a permeation source and a gas-phase mixture (3.1 ppmv in N₂) implies that the UV absorption cross section is high by 5-10% or that there were contaminants in both calibration sources. NH₃ is one of the more important reactive nitrogen species in the atmosphere-biosphere system and is thermodynamically one of the more difficult to convert. Compounds considered NO_y species, such as nitric acid, acetyl peroxy nitrates, and alkyl nitrates were not studied in this work (aside from NO₂), since they are known to be converted at high efficiency on precious metal (Fahey et al., 1986) or molybdenum oxide (Winer et al., 1974) catalysts. The resulting uncertainties in the N_r measurement are estimated to be $\pm 10\%$ based on comparisons of measured NO signals to individual N_r compound calibrations.

The conversion of nitrous oxide (N₂O) is a potential interference in the N_r method as N₂O is not typically considered a reactive nitrogen compound in the troposphere. Several experiments were conducted to determine the extent of this potential interference using a 10.1 ppmv N₂O standard. The resulting conversion efficiency ranged from 0.03% to 0.05% in dry and humidified air respectively. These can be considered upper limits for this interference as we cannot be completely sure that there were no N_r contaminants (e.g. NO₂) in the N₂O standard. N₂O is a potential interference that is discussed in Sect. 2.2.1, though in this instance this the conversion efficiency upper limit determined for this instrument is a negligible interference in the N_r measurements in ambient air or zero air matrices, and likewise will not be significant in biomass burning sources given that N₂O enhancements in fresh biomass smoke are generally not observed or contribute minimally to total nitrogen (Griffith et al., 1991). N₂O emissions from other sources (e.g. natural and anthropogenic agricultural sources, fossil fuel combustion, or animal waste) can be significant, therefore the interference from N₂O conversion must be considered. O₃ is another potential source of gas-phase interference due to the decomposition of O₃ to O₂ + O, followed by reaction of O with N₂O at high temperature to form NO. However, the NO production in the O + N₂O reaction is an approximately 20% channel with a net rate constant of approximately 1×10^{-15} cm³ molecule⁻¹ s⁻¹ at 750°C (NIST 2017). If all the O atoms from 70 ppbv of O₃ were available for reaction with an ambient level of N₂O (340 ppbv), then the 0.1 sec residence time in the convertor

Formatted: Subscript

Formatted: Subscript

Formatted: Subscript

would result in approximately 28 pptv of NO, an upper limit that is ~~clearly~~ generally a negligible amount in almost any atmospheric context ~~except in remote regions~~.

3.2 Nr particle measurements

3.2.1 Nr system set-up and response

The atomizer output was diluted with particle-free nitrogen and ultra-pure zero air, therefore, the N_r measurement should theoretically be attributed to particles only since no detectable gas-phase nitrogen is added to the sample stream. However, equilibration within the sample lines may result in outgassing and formation of gas-phase compounds affecting total N_r detection. Fig. 3(a) shows the initial response of the N_r system in cleaned inlets for NaNO_3 . The N_r mass signal tracks the CPC-derived aerosol mass features closely as the aerosol source concentrations fluctuate. Additionally, as different particle sizes are selected by the DMA for $(\text{NH}_4)_2\text{SO}_4$ (Fig. 3(b)), changes in the total N_r response is fast and precisely tracks the changes in the CPC signal. The potential gas-phase constituents equilibrating in the lines from aerosols in this study include HNO_3 , HCl , and NH_3 . If these compounds formed before reaching the N_r catalyst it is likely adsorption and desorption from inlets and tubing surfaces would occur (e.g. Neuman et al., 1999; Yokelson et al., 2003). As an example, the presence of NH_3 in Fig. 3(b) (or HNO_3 in nitrate containing particles) would be indicated by a delayed and lengthened rise/fall in the N_r response with sudden changes to the input concentrations. However, the total N_r response precisely tracks the CPC signal on rapid timescales (a few seconds) suggesting that gas-phase NH_3 was not present in significant quantities. In experiments at exceptionally high aerosol loading of $(\text{NH}_4)_2\text{C}_2\text{O}_4$ (up to several ppmv of total N_r , i.e., several thousand $\mu\text{g m}^{-3}$) N_r signal “tailing” was observed suggesting that NH_3 was scavenging to the walls of the inlet before the heated quartz tubing.

Marx et al. (2012) reported calculated conversion efficiencies in air sampled from a small chamber for NaNO_3 , NH_4NO_3 , and $(\text{NH}_4)_2\text{SO}_4$ to be 78, 142, and 91%, respectively. The authors suggested the overestimation of NH_4NO_3 was a result of its semi-volatile properties under ambient conditions that led to the formation of gaseous NH_3 and HNO_3 in the chamber. For these reasons, we limit the background artifacts and volatilization effects that may have occurred during chamber filling and sampling in Marx et al. (2012) by sampling immediately following solution atomization through conductive tubing at relatively high sample flow rates. Additionally, we use a DMA to size-select the atomized polydisperse aerosol to evaluate the particle conversion efficiency at several different diameters (100 – 600 nm in 50 nm increments) to investigate the volatilization effects and conversion efficiencies of smaller particles for the extended list of N_r -containing aerosols studied in our work.

3.1.2 Nr system set-up and response

~~The atomizer output was diluted with particle free nitrogen and ultra pure zero air, therefore, the N_r measurement should theoretically be attributed to particles only since no detectable gas-phase nitrogen is added to the sample stream. However, equilibration within the sample lines may result in outgassing and formation of gas-phase compounds affecting total N_r detection. Fig. 3(a) shows the initial response of the N_r system in cleaned inlets for NaNO_3 . The N_r mass signal tracks the CPC-derived aerosol mass features closely as the aerosol source concentrations~~

Formatted: Line spacing: single

fluctuate. Additionally, as different particle sizes are selected by the DMA for $(\text{NH}_4)_2\text{SO}_4$ (Fig. 3(b)), changes in the total N_r response is fast and precisely tracks the changes in the CPC signal. The potential gas-phase constituents equilibrating in the lines from aerosols in this study include HNO_3 , HCl , and NH_3 . If these compounds formed before reaching the N_r catalyst it is likely adsorption and desorption from inlets and tubing surfaces would occur (e.g. Neuman et al., 1999; Yokelson et al., 2003). As an example, the presence of NH_3 in Fig. 3(b) (or HNO_3 in nitrate-containing particles) would be indicated by a delayed and lengthened rise/fall in the N_r response with sudden changes to the input concentrations. However, the total N_r response precisely tracks the CPC signal suggesting that gas-phase NH_3 was not present in significant quantities. In experiments at exceptionally high aerosol loading of $(\text{NH}_4)_2\text{C}_2\text{O}_4$ (up to several ppmv of total N_r , i.e., several thousand $\mu\text{g m}^{-3}$) N_r signal “tailing” was observed suggesting that NH_3 was scavenging to the walls of the inlet before the heated quartz tubing.

Marx et al. (2012) reported calculated conversion efficiencies in air sampled from a small chamber for NaNO_3 , NH_4NO_3 , and $(\text{NH}_4)_2\text{SO}_4$ to be 78, 142, and 91%, respectively. The authors suggested the overestimation of NH_4NO_3 was a result of its semi-volatile properties under ambient conditions that led to the formation of gaseous NH_3 and HNO_3 in the chamber. For these reasons, we limit the background artifacts and volatilization effects that may have occurred during chamber filling and sampling in Marx et al. (2012) by sampling immediately following solution atomization through conductive tubing at relatively high sample flow rates. Additionally, we use a DMA to size select the atomized polydisperse aerosol to evaluate the particle conversion efficiency at several different diameters (100–600 nm in 50 nm increments) to investigate the volatilization effects and conversion efficiencies of smaller particles for the extended list of N_r -containing aerosols studied in our work.

3.1.32.2 N_r -particle conversion efficiency Challenges using the DMA/SMPS to determine N_r -particle conversion efficiency

The voltage scanning (SMPS) function of the DMA and number concentration measurements by the CPC is a conventional method to determine particle size distributions, and for calculating particle mass from total volume and density, assuming spherical particles. For the total nitrogen measurements, the total particle-bound N_r mixing ratios were retrieved and converted to mass concentrations for each corresponding salt. Figures 4(a-d) show the SMPS-calculated vs N_r -measured mass concentrations ($\mu\text{g m}^{-3}$) for particles of different composition and diameter. The plots show that a strong correlation ($R^2 > 0.98$) and good agreement was obtained for smaller particles (50–200 nm) with slopes ranging from 0.86–0.97, while for larger particles (≥ 250 nm) the mass calculated values from the SMPS-derived distributions were sometimes as much as >50% too high. The R^2 for all particles including ≥ 250 nm ranged from 0.71–0.85 with slopes of 1.08–1.36.

For larger particles, we used a UHSAS to determine the size distribution of multiply-charged species exiting the DMA. The SMPS inversion-derived size distributions were generally broader than the UHSAS size distributions, though agreement improved at increased scan times. Small differences in the size distribution recovered from the voltage scans at larger diameters (> 200 nm) affected the mass distribution considerably because particle mass scales with diameter cubed. A possible explanation is that we are not correctly accounting for the delay time from the DMA exit to the CPC, therefore the particle counts did not correspond to the correct size designated from voltage scanning

and this likely skewed the size distribution relative to the true distribution (Collins et al., 2002). Methods for limiting these effects exist (Russell et al., 1995; Collins et al., 2002) including slower voltage scan rates. However, our results demonstrate the added challenges in particle mass determination using estimated size distributions from the SMPS method. However, our results demonstrate the added challenges in particle mass determination using estimated size distributions from the SMPS method. Other aerosol measurement techniques (e.g. the Particle Time of Flight mode of the Aerosol Mass Spectrometer; DeCarlo et al., 2006) directly measure size distributions or instead measure polydisperse aerosol and the instrument and inversion algorithm corrections required using the SMPS are avoided. Therefore, we instead For the remaining discussion, we measure the size distributions directly using the UHSAS with particle concentration measurements (by either the CPC or UHSAS) to evaluate the N_r particle conversion in the N_r system.

3.2.3 Determining N_r -particle conversion efficiency using a DMA and UHSAS

For the aerosol mass concentrations ($\mu\text{g m}^{-3}$) calculated using UHSAS particle size distributions, we refer to these values as UHSAS calculated mass. Comparisons of the mass directly measured as N_r versus UHSAS calculated mass concentrations for atomized solutions of NaNO_3 , $(\text{NH}_4)_2\text{SO}_4$, NH_4Cl , and $(\text{NH}_4)_2\text{C}_2\text{O}_4$ are shown in Fig. 5 with orthogonal distance regression lines with slopes that range from 0.910 – 1.06 for concentrations from ~0–70 $\mu\text{g m}^{-3}$. The instruments are highly correlated ($R^2 = 0.90 - 0.99$) and the fits indicate that for the salts tested there is quantitative conversion of particulate nitrogen, to within the combined uncertainties of the methods, independent of diameter (range: 100 – 600 nm). More detailed particle conversion efficiencies by size are shown in Table 2 for each aerosol tested. On average across all size ranges the results indicate $97 \pm 7\%$, $101 \pm 5\%$, $100 \pm 10\%$, and $93 \pm 5\%$ particle conversion efficiencies for NaNO_3 , $(\text{NH}_4)_2\text{SO}_4$, NH_4Cl , and $(\text{NH}_4)_2\text{C}_2\text{O}_4$, respectively. The largest deviation from the one-to-one line occurred for $(\text{NH}_4)_2\text{C}_2\text{O}_4$, which may imply some ammonia loss, though the agreement is generally still within 10% for most particle sizes.

For the case of NH_4NO_3 , the UHSAS measured size distribution peaked at significantly lower diameters than expected based on the DMA size selection. This difference has been reported previously (Cai et al., 2008; Womack et al., 2017), though to a lesser extent (~8%) than observed here (up to 30%). Possible explanations for these differences could include vaporization/evaporation effects, residual water in the particles, surface effects, or differences in electrical mobility diameter and geometric diameter due to non-sphericity as discussed in DeCarlo et al. (2004). For these reasons, we made no attempt to characterize NH_4NO_3 behavior in either the DMA or UHSAS and refer to Sect. 3.2.4.1 for mass concentration comparisons of polydisperse aerosol measured using separate mass measurement techniques (both the N_r system and PILS-ESI/MS). It is worth noting that NH_4NO_3 is one of the more volatile compounds included in this study and it is reasonable to expect similar particle conversion efficiencies in the N_r system catalysts for NH_4NO_3 as the other species tested (Table 2).

3.3 Carbon conversion efficiency of Pt catalyst

The high-temperature platinum catalyst should quantitatively convert carbon containing species to CO_2 in the presence of air. Therefore, the addition of a CO_2 analyzer to the system as described in Sect. 2.1.2 allows for

Formatted: Heading 2, Left, Indent: First line: 0", Line spacing: single

Formatted: Subscript

Formatted: Subscript

simultaneous measurements of N_r and C_v . Gas-phase carbon conversion across similar precious metals has been studied previously (e.g. Veres et al., 2010). The efficient conversion of gas-phase C-compounds in our catalyst system was confirmed using a CO standard in air, and a combination CO_2 , CO, CH_4 standard in air. The following discussion focuses on the conversion of particle-phase organic compounds (OC). The efficient conversion of N_r -containing particles was demonstrated in Sect. 3.2.2 for the range of N oxidation states and should extend to other N_r -containing particles, we expect that the resulting N_r and C_v signals from each detector will be in proportion by dividing the result by the number of carbon and nitrogen atoms in the parent molecule to give the standard concentration on a molar basis. Polydisperse particulate OC was generated from solution following an N_2 purge to eliminate carbonate from the solution. Aerosol particles from solutions of anthranilic acid ($C_7H_7NO_2$, 2-aminobenzoic acid, Sigma Aldrich), threonine ($C_4H_9NO_3$, 2-amino-3-hydroxybutanoic acid, Sigma Aldrich), tryptophan ($C_{11}H_{12}N_2O_2$, 2-amino-3-indolylpropanoic acid, Sigma Aldrich), and quinine ($C_{20}H_{24}N_2O_2$, Sigma Aldrich) were tested. These compounds were chosen based on their water solubility to avoid the use of organic solvents. An example of the N_r and C_v response is shown in Fig. 7 for threonine (see Fig. S1 for additional compounds). The relative difference between the N_r and C_v measured concentrations (up to several hundred ppbv) is less than 10%, which is within the propagated uncertainties of the CO_2 calibration standards and both detection methods. We conclude that the N_r catalyst with a CO_2 detector in parallel can be used as a total carbon measurement system and would be useful to establish instrument calibrations for carbon-containing aerosol. The system is currently limited to calibration of compounds in zero air matrices because ambient levels of the common gas-phase carbon compounds CO_2 , CO, and CH_4 are high.

3.1.4 N_r measurements of biomass burning emissions

As an example of both gas and particle measurements using the N_r system, we follow with a brief discussion of N emissions from biomass burning. The primary gaseous N-compounds in biomass burning plumes include NO, NO_2 , N_2 , NH_3 and to a lesser extent HCN, CH_3CN , HONO, HNCO (Lobert et al., 1990; Lobert et al., 1991; Kuhlbusch et al., 1991; McMeeking et al., 2009; Burling et al., 2010; Stockwell et al., 2014; 2015) and other N_r -containing gases. Figure 67 shows results obtained from a representative fire (Fire 047) from the Fire Influence on Regional and Global environments Experiment (FIREX) 2016 Missoula Fire Lab study (<https://www.esrl.noaa.gov/csd/projects/firex/>). Figure 67(a) shows the co-measured N_r and NO concentrations (ppmv). The majority of the N_r system's response is due to the sum of gas-phase N_r -constituents that were measured by a Fourier transform infrared spectrometer (FTIR; Selimovic et al., 2017, 2018), an H_3O^+ chemical ionization mass spectrometer (Koss et al., 2017, 2018), and a broadband cavity enhanced extinction spectrometer (Min et al., 2016) (Fig. 67(b)). At the beginning of the burn (pre 10:23 AM) the average relative percent difference between the total nitrogen signal and the sum of individually measured gas-phase compounds is ~16%, which is less than the combined error of the individual measurements. There is greater disagreement shown in Fig. 67(c) (difference is up to ~1 ppmv; up to ~50% relative percent difference) during other stages of the fire. The modified combustion efficiency (MCE) is a measure to estimate the relative contribution of flaming and smoldering combustion that occurred over the course of a fire, where the MCE is defined as the ratio of $\Delta CO_2 / (\Delta CO_2 + \Delta CO)$ (Yokelson et al., 1996). A higher MCE value (approaching 0.99) designates relatively pure flaming combustion (more complete oxidation) and a lower MCE (~ 0.75–0.84) designates more smoldering

combustion. We have shown in our laboratory experiments that there is quantitative N_r particle conversion across the N_r catalyst, therefore, it is likely possible that the residual signals are due to particulate N-containing compounds. Particulate ammonium may contribute to the excess N_r signal measured during periods dominated by smoldering combustion ($MCE < 0.90$). The oxidized N-containing gas phase species are relatively more abundant during the initial part of the fire, so while particulate nitrate likely could account for some N_r signal during the flaming dominated stages as shown in Fig. 6. By confirming particulate N_r -conversion in this system, it is possible that a total N budget can be reconstructed for additional laboratory fires measured during the FIREX laboratory study where individual particle phase N_r data are available.

3.1.5 Carbon conversion efficiency of Pt catalyst

The high-temperature platinum catalyst (Fig. 1) in the N_r instrument should quantitatively convert carbon containing species to carbon dioxide (CO_2) in the presence of air. Gas phase carbon conversion across similar precious metals has been studied extensively (see for example the Pt catalyst used in Veres et al., 2010). Therefore, adding a CO_2 analyzer to the configuration allows for simultaneous measurements of N_r and C_y .

For the following experiments, the total flow through the Pt catalyst was increased slightly ($\sim 1.5 \text{ sL min}^{-1}$) and was then split after the Pt and before the MoOx catalyst, with the smaller flow (0.5 sL min^{-1}) directed through the LICOR 6251 (LI 6251; Lincoln, NE) CO_2 analyzer, and the main flow directed through the MoOx catalyst and the $NO-O_3$ chemiluminescence detector. The LICOR instrument was internally referenced to scrubbed zero air. The conversion of compounds that contain both N and C atoms can then be measured simultaneously using the $NO-O_3$ chemiluminescence detector and LI 6251 detector in parallel. At ambient CO_2 levels, it is challenging to retrieve reliable measurements since the signal relative to the background abundance of CO_2 is small. The approach described here relies on using ultra-pure air for aerosol generation and carrier gas flow, therefore ambient air is eliminated. The LI 6251 was calibrated with sub-5 ppm CO_2 standards (Scott-Marin Inc., Riverside, CA) in ultra-pure air. Due to the low signal levels and the uncertainty of the low concentration CO_2 standards, the overall accuracy of the CO_2 measurements present in this work up to 1 ppmv is $\pm 10\%$ for 10-second averages.

The efficient conversion of gas-phase C compounds in our catalyst system was confirmed using a CO standard in air, and a combination CO_2 , CO, CH_4 standard in air. The following discussion focuses on the conversion of particle-phase organic compounds (OC). The efficient conversion of N_r containing particles was demonstrated in Sect. 3.1.3 for the range of N oxidation states. We are confident these results extend to other N_r containing particles, which is supported by the extensive list of N_r gases efficiently converted as shown in Table 1. Therefore, we expect that the resulting N_r and C_y signals from each detector will be in proportion by dividing the result by the number of carbon and nitrogen atoms in the parent molecule to give the standard concentration on a molar basis. Polydisperse particulate OC was generated from solution following an N_2 purge to eliminate carbonate from the solution. Aerosol particles from solutions of anthranilic acid ($C_7H_7NO_3$; 2-aminobenzoic acid, Sigma Aldrich), threonine ($C_4H_9NO_3$; 2-amino-3-hydroxybutanoic acid, Sigma Aldrich), tryptophan ($C_{11}H_{12}N_2O_2$; 2-amino-3-indolylpropanoic acid, Sigma Aldrich), and quinine ($C_{20}H_{24}N_2O_5$; Sigma Aldrich) were tested. These compounds were chosen based on their water solubility to avoid the use of organic solvents. An example of the N_r and C_y response is shown in Fig. 7 for threonine

(see Fig. S1 for additional compounds). The relative difference between the N_r and C_r measured concentrations (up to several hundred ppbv) is less than 10%, which is within the propagated uncertainties of the CO_2 calibration standards and both detection methods.

Initial tests with $(NH_4)_2C_2O_4$ proved more challenging as the low C number required large polydisperse aerosol loadings (several ppmv) to be measured reliably by the LICOR. During these instances, surface effects reduced the total N_r signal, which likely resulted from NH_3 scavenging to the walls of the transfer lines or quartz tubing. We conclude that the N_r system with a CO_2 detector in parallel can be used as a total carbon measurement system and would be useful to establish instrument calibrations for carbon-containing aerosol. The system is currently limited to calibration of compounds in zero air matrices because ambient levels of the common gas phase carbon compounds CO_2 , CO , and CH_4 are high.

3.24 Comparisons with the PILS-ESI/MS Application to calibrate the PILS-ESI/MS

3.2.1 N_r system as an aerosol mass measurement method

Here we demonstrate the capability of the total nitrogen system as an independent calibration method for [other aerosol](#) measurement systems. N_r measurements of laboratory generated single-component inorganic and organic aerosol particles were used to characterize [a novel configuration coupling a PILS with electrospray ionization interface followed by mass spectrometric detection the PILS-ESI/MS](#). The strength of using the N_r system to calibrate the PILS-ESI/MS [and other aerosol mass instruments](#) is that it is a direct method to calibrate the entire coupled on-line system. The current calibration approach [for nearly all detectors used with the PILS](#) involves liquid-phase standards to calibrate the [ESI/MS detection method](#) independently from the PILS.

The inorganic salts selected for [this study the comparison between \$N_r\$ and the PILS-ESI/MS instruments](#) all contained N atoms, either in the cation, anion, or both. The total N_r measured as NO (in ppbv) included all the N atoms atomized from the single-component solution. Dividing the total N_r measurement by the number of N atoms in the parent molecule gives the standard concentration (in ppbv) of the corresponding anion (e.g. Cl^- , NO_3^- , SO_4^{2-} , $C_2O_4^{2-}$). The mixing ratios (in ppbv) are converted to $\mu g m^{-3}$ from the molecular weight of the corresponding anion. We refer to these mass concentrations as “X measured as equivalent N_r ” in the remainder of the text, where X is the corresponding anion of the aerosol particle. The anion mass calculated in this way was only necessary when comparing directly to PILS-ESI/MS measurements of [ammonium salts of](#) nitrate, sulfate, chloride, and oxalate.

3.2.1.1 N_r and PILS-ESI/MS mass concentration comparisons

[In coupling an aerosol collection technique \(PILS\) with an electrospray ionization source, water-soluble aerosol particles are speciated in real time.](#) To compare to the calibration approaches [through using](#) liquid phase standards described in Sect 2.1.2.3 for the PILS-ESI/MS we performed particle mass comparisons using these methods with anion-specific mass concentrations derived from the N_r measurement system. A single-component aerosol was used to minimize complex matrix effects including ion suppression/enhancement common in ESI.

An example of the N_r system and PILS-ESI/MS co-sampling a laboratory generated polydisperse aerosol stream is shown in Fig. 8. Here we did not size-select aerosols, but measured all particle sizes below a 2.5 μm cut-off

Formatted: Indent: First line: 0"

Formatted: Subscript

(URG cyclone, Chapel Hill, NC). There are two reasons for this experimental set-up: (1) Generating a sufficient aerosol mass concentration to calibrate the PILS-ESI/MS was challenging because it requires a minimum flow of 11 L min⁻¹, while the DMA output flow is <1 L min⁻¹, therefore the DMA aerosol flow required a large dilution. ~~Because a greater aerosol particle mass could be realized by directly sampling the polydisperse output of the atomizer, our analysis focuses on comparisons between N_r and PILS-ESI/MS without using the DMA size selection.~~ (2) Conventionally, the PILS instrument samples with a cyclone with a 1 or 2.5 µm cutoff, which is similar to other mass measurement instruments including the aerosol mass spectrometer (AMS) and filter collection.

Figure 8 shows the aerosol nitrate (blue) trace from NaNO₃ particles measured by the PILS-ESI/MS shifted in time to account for the system delay time so that it aligns with the relatively steady concentration periods with the N_r trace (black). The PILS-ESI/MS had a response time of roughly 4-5 min in its current configuration. Several stages in the PILS system included mixing volumes (e.g. syringe pumps and mixing vessels) that prevented rapid response to rapidly changing concentrations and smeared the response. For instrument comparisons 60 s data were averaged and compared during periods with relatively steady concentrations (generally lasting 5- 10 min). Examples of PILS-ESI/MS traces aligned such that initial response of both instruments coincide are shown in Fig. S2.

The correlation plot of PILS-ESI/MS to equivalent anion mass measured as N_r for each aerosol-type (NaNO₃, (NH₄)₂SO₄, NH₄Cl, and NH₄NO₃) is shown in Fig. 9(a-d). The concentrations ranged from ~10–120 µg m⁻³ and the standard linear regression fits for each aerosol type are included in Fig. 9, and were highly correlated with a R² = 0.99. For (NH₄)₂SO₄, the concentration exceeded the linear dynamic range of the PILS-ESI/MS for sulfate (see Fig. S2(a); > 130 µg m⁻³) as determined by liquid-standard calibration curves. The linear range of ESI is limited at high concentrations due to limited surface sites available for ionization (Tang et al., 2004). For this reason values outside the linear dynamic range of the PILS-ESI/MS (> 130 µg m⁻³) for sulfate were excluded from the linear regression fit. NH₄NO₃ shows a similar, less pronounced trend, however, it is still included in the regression plot as it was difficult to isolate whether this was analyte suppression during electrospray ionization or a linear dynamic range issue. Based on the regression fits in Fig. 9, the difference between the PILS-ESI/MS and N_r system for each inorganic component is less than 6%. The uncertainty in the ESI signal varies by compound and averaging time, however from the tests described here the maximum uncertainty is estimated ~15%. Combining this uncertainty with the uncertainty in the ESI calibrations (maximum ± 10%), the air and liquid flow rate (both ~± 4%), and dilution (~± 5%) in quadrature gives a total maximum uncertainty associated with mass measurements of ± 20%. So while the slope of the correlations of the two instruments (based on 60 s averages during periods with constant concentrations) shows a relative difference of less than ~6%, the uncertainty in the PILS/ESI measurement of single component aerosols is closer to ~ 20% and could be greater if the transmission and ionization efficiencies of the ESI differ from the efficiencies present during calibration periods. This uncertainty is greater than the uncertainty (± 10 %) reported for the PILS-IC instrument for ionic species in Weber et al. (2001) but lower than the AMS uncertainty for nitrate (33 %) and sulfate (35%) estimated by Bahreini et al. (2009), though the AMS has a much faster time response.

Even though greater aerosol particle mass could be produced by directly sampling the polydisperse output of the atomizer, our analysis also included measurements using the DMA size-selected output. During these tests the flow was divided between the N_r system, CPC, UHSAS, and PILS-ESI/MS with a large dilution flow that resulted in

turbulent mixing ($Re > 4000$). The CPC and UHSAS particle number concentrations showed improved agreement with turbulent mixing compared to earlier differences up to 10% at high concentrations discussed in Sect. 2.3.2.2 and were within a few percent of each other. Examples of the real-time temporal profiles for these measurements are shown in Fig. 10(a-d) with the PILS-ESI/MS time offset by several minutes to account for its delayed response. The calculated and measured aerosol mass time traces in Fig. 10 show agreement for all measurement techniques tested in this study. The figures indicate that the PILS-ESI/MS was not given sufficient time to rise to a steady constant concentration for the first diameter selected. This is confirmed by Fig. 10(b) during which 200 nm particles were size selected twice in succession with the first selection lasting only ~2 min before flushing with water quickly followed by a longer period of sampling at the same diameter. The PILS-ESI/MS concentration during this longer sampling period does reach the expected concentration as indicated by the N_r (black) and CPC (blue) concentrations. The time-series of oxalate in Fig. 10(d) shows agreement for the equivalent N_r and PILS-ESI/MS measured mass indicating these same calibration methods are effective for organic compounds, although the UHSAS was not sampling during this experiment. We conclude that the PILS-ESI/MS quantitatively measures single component inorganic aerosol for a range of sizes, however, the low particle throughput hindered our ability to evaluate the quantitative abilities of the PILS-ESI/MS system for particles < 200 nm diameter.

These results establish the quantitative abilities of this novel configuration (PILS-ESI/MS) for sampling simple single-component laboratory generated aerosol. ~~However, our current ESI/MS calibration methods are sensitive to the experimental conditions, which must be precisely maintained during ESI calibrations and throughout the entire sampling period. Changes in flow rate, interface positioning, or solvent composition have significant impacts on both the transmission and ionization efficiency ultimately effecting pre-determined ESI calibration factors. We evaluated this previously uncharacterized mass measurement technique using both traditional particle number size distribution measuring systems and the total N_r mass measurement system. In general, PILS characterization has been limited to theoretical predictions or experimental comparisons that involve coupling the PILS with a mass analyzer (e.g. IC; Orsini et al., 2003; Sorooshian et al., 2006). Here we show experimentally that the N_r system can be used as a mass calibration method for pure N_r -containing polydisperse aerosol. Calibrating the ESI/MS using direct injection of liquid standards combined with mass concentrations collected by the PILS is a valid approach for quantifying inorganic components of aerosols, which likely extends to several organics as demonstrated by oxalate. However, these ESI/MS calibrations are sensitive to the experimental conditions, which must be precisely maintained during ESI calibrations and throughout the entire sampling period. Changes in flow rate, interface positioning, or solvent composition have significant impacts on both the transmission and ionization efficiency ultimately effecting pre-determined ESI calibration factors. Additionally, PILS characterization has been limited to theoretical predictions or experimental comparisons that involve coupling the PILS with a mass analyzer (e.g. IC; Orsini et al., 2003; Sorooshian et al., 2006). Here we introduced a new method for calibrating the entire PILS-ESI/MS coupled system using N_r -equivalent mass measurements of Cl^- , NO_3^- , SO_4^{2-} , $C_2O_4^{2-}$ from N_r -containing particles.~~

4.5 Summary and conclusions

We report the successful application of a total reactive nitrogen (N_r) system for conversion of gas-phase and particle-bound N_r -compounds. The N_r system was tested using laboratory-generated monodisperse aerosol from solutions of $(NH_4)_2SO_4$, NH_4Cl , $NaNO_3$, and $(NH_4)_2C_2O_4$. The particle conversion efficiency of each compound was calculated at each size-selected diameter by the ratio of the concentration measured as N_r to mass concentrations calculated from number concentration and size distribution measurements using a CPC and UHSAS. Overall, the particle conversion efficiency for a selection of N_r -containing aerosols ranged from 93–101% with an overall estimated uncertainty of ~10%. The N_r - particles tested in these experiments span the range of N oxidation states, and therefore we are confident these results extend to other N_r -containing particles. Most catalyst-based N_r systems measure total gas-phase N_r -only, individual N_r -compounds (e.g. NH_3), or ignore the contribution of particulate N_r to total signal completely. However, it is useful to measure the total unspiciated N_r signal, which includes both gases and particles, to improve our understanding of total N-emissions and their deposition, loss, and availability in ecosystems (e.g. McCalley and Sparks, 2009). We have presented a rapid, robust measurement technique that quantitatively measures particle N_r mass that allows for accurately interpreting ambient measurements, and allows improved mass closure of the N-budget to be constructed for the 2016 Fire Sciences Laboratory measurements of wildfire emissions. Future applications of this custom system aim to distinguish gas- and particle-phase nitrogen contributions to total measured N_r signal using upstream filters and denuders.

Additional characterization tests showed the platinum catalyst in the N_r system quantitatively converts both gaseous- and particulate-organic carbon (OC) to CO_2 to within the propagated uncertainties of each detection method ($\pm 10\%$ each). The resulting N_r and C_y signals from each detector are in proportion to the number of carbon and nitrogen atoms in the parent molecule. In order for this to be a reliable total particulate carbon measurement system under ambient conditions, a highly accurate and precise CO_2 measurement system is imperative to measure the signal above ambient CO_2 , CO, and CH_4 backgrounds. Alternatively, ambient gas-phase constituents could be effectively eliminated from the sampling matrix. For these reasons, the application of the system is currently limited to calibration of single-component OC- and/or N_r -containing particles.

After establishing efficient conversion of N_r -particles, we experimentally demonstrated that this the N_r conversion technique can be used to calibrate aerosol particle mass measurement methods when sampling pure N_r -containing polydisperse aerosol. The N_r equivalent mass measurements of pure atomized polydisperse aerosol showed an agreement of within $\pm 6\%$ with the PILS-ESI/MS measurements of the corresponding anion for the salts $(NH_4)_2SO_4$, NH_4Cl , $NaNO_3$, and NH_4NO_3 . There is a clear advantage to calibrating the entire PILS-ESI/MS system altogether as this avoids complications arising from calibrating the ESI/MS and PILS independently. We conclude that the N_r system is an effective measurement technique that can be used to directly calibrate aerosol mass measurement instruments. With this direct mass calibration method, complications that arise due to optical (e.g. refractive index) and physical properties (e.g. morphologies) in particle number calibration methods are avoided. Additionally, this method is an on-line technique that provides a rapid measurement of particle mass unlike off-line mass measurement methods such as filter analyses. The N_r converter described followed by NO and CO_2 detection is a viable new approach for calibrating aerosol mass instrumentation for both N-containing and organic carbon particles.

Formatted: Subscript

1 **Data availability**

2 The data from the laboratory tests are available on request. Data from the 2016 Missoula Fire lab are available here:
3 <https://esrl.noaa.gov/csd/groups/csd7/measurements/2016firex/FireLab/DataDownload/index.php?page=/csd/groups>
4 /[csd7/measurements/2016firex/FireLab/DataDownload/](https://esrl.noaa.gov/csd/groups/csd7/measurements/2016firex/FireLab/DataDownload/)

5 **Author contribution**

6 CES wrote the paper with help from JMR. CES performed the particle calibrations with help from RAW and AK.
7 JMR and YL built the N_r catalyst and performed the tests to verify gas-phase conversion of N_r species. AM advised
8 on operation of the PILS. BW, RKT, and CES designed, constructed, and characterized the ESI interface. VS, RJY,
9 KJZ, CW, and KS made measurements of individual N- species during the FIREX campaign.

10 **Competing interests**

11 The authors declare no competing interests or other conflicts of interest.

12 **Disclaimer**

13 Mention of commercial products is for identification purposes only and does not imply endorsements.

14 **Acknowledgements**

15 This work was supported by NOAA's Climate and Health of the Atmosphere initiatives. C.S. acknowledges support
16 from the National Research Council Research Associateship Program. B. W. was supported by the Kościuszko
17 Foundation Program for Advanced Study, Research and/or Teaching in the United States 2014-2015. A. K. is
18 supported by the Austrian Science Fund FWF's Erwin Schrodinger Fellowship J-3613. The FIREX Fire Lab study
19 was supported in part by the NOAA Climate Office's Atmospheric Chemistry, Carbon Cycle, and Climate program.
20 We thank Dr. Brad Hall for the use of his nitrous oxide standard. We thank S. N. Anthony and the Jarrold group for
21 giving us an ion carpet board for the ESI interface. We thank Matthew Coggon, Abigail Koss, and Joost de Gouw,
22 for their H₃O⁺ CIMS data and Steven Brown for his [airborne](#)-cavity enhanced spectrometer data. We would like to
23 thank Katherine Manfred, Alessandro Franchin, and Charles Brock for their useful discussions.

24 **References**

25 Anthony, S. N., Shinholt, D. L., and Jarrold, M. F.: A simple electrospray interface based on a DC ion carpet, *Int. J.*
26 *Mass Spectrom.*, 371, 1-7, doi:10.1016/j.ijms.2014.06.007, 2014.

27 Bahreini, R., Ervens, B., Middlebrook, A. M., Warneke, C., de Gouw, J. A., DeCarlo, P. F., Jimenez, J. L., Brock, C.
28 A., Neuman, J. A., Ryerson, T. B., Stark, H., Atlas, E., Brioude, J., Fried, A., Holloway, J. S., Peischl, J., Richter,
29 D., Walega, J., Weibring, P., Wollny, A. G., and Fehsenfeld, F. C.: Organic aerosol formation in urban and
30 industrial plumes near Houston and Dallas, Texas, *J. Geophys. Res.*, 114, D00F16, doi:10.1029/2008JD011493,
31 2009.

1 Bauer, S. E., Koch, D., Unger, N., Metzger, S. M., Shindell, D. T., and Streets, D. G.: Nitrate aerosols today and in
2 2030: a global simulation including aerosols and tropospheric ozone, *Atmos. Chem. Phys.*, 7, 5043-5059,
3 doi:10.5194/acp-7-5043-2007, 2007.

4 Bellouin, N., Rae, J., Jones, A., Johnson, C., Haywood, J., and Boucher, O.: Aerosol forcing in the Climate Model
5 Intercomparison Project (CMIP5) simulations by HadGEM2-ES and the role of ammonium nitrate, *J. Geophys.*
6 *Res.*, 116, D20206, doi:10.1029/2011JD016074, 2011.

7 Benedict, K. B., Prenni, A. J., Carrico, C. M., Sullivan, A. P., Schichtel, B. A., and Collett Jr., J. L.: Enhanced
8 concentrations of reactive nitrogen species in wildfire smoke, 148, 8-15, doi:10.1016/j.atmosenv.2016.10.030, 2017.

9 Bohren, C. F., and Huffman, D. R.: Absorption and scattering of light by small particles, Wiley, New York, 1983.

10 Breitenbach, L. P. and Shelef, M.: Development of a method for the analysis of NO₂ and NH₃ by NO-measuring
11 instruments, *J. Air Pollut. Contr. Assoc.*, 23, 128-131, doi:10.1080/00022470.1973.10469752, 1973.

12 Burling, I. R., Yokelson, R. J., Griffith, D. W. T., Johnson, T. J., Veres, P., Roberts, J. M., Warneke, C., Urbanski,
13 S. P., Reardon, J., Weise, D. R., Hao, W. M., and de Gouw, J.: Laboratory measurements of trace gas emissions
14 from biomass burning of fuel types from the southeastern and southwestern United States, *Atmos. Chem. Phys.*, 10,
15 11115–11130, doi:10.5194/acp-10-11115-2010, 2010.

16 Cai, Y., Montague, D. C., Mooiweer-Bryan, W., and Deshler, T.: Performance characteristics of the ultra high
17 sensitivity aerosol spectrometer for particles between 55 and 800 nm: Laboratory and field studies, *J. Aerosol Sci.*,
18 39, 759-769, doi:10.1016/j.jaerosci.2008.04.007, 2008.

19 Canagaratna, M. R., Jayne, J. T., Jimenez, J. L., Allan, J. D., Alfarra, M. R., Zhang, Q., Onasch, T. B., Drewnick, F.,
20 Coe, H., Middlebrook, A., Delia, A., Williams, L. R., Trimborn, A. M., Northway, M. J., DeCarlo, P. F., Kolb, C.
21 E., Davidovits, P. and Worsnop, D. R.: Chemical and microphysical characterization of ambient aerosols with the
22 [aerodyne-Aerodyne](#) aerosol mass spectrometer, *Mass Spectrom. Rev.*, 26, 185–222, doi:10.1002/mas.20115, 2007.

23 Cape, J. N., Cornell, S. E., Jickells, T. D., and Nemitz, E.: Organic nitrogen in the atmosphere-Where does it come
24 from? A review of sources and methods, *Atmos. Res.*, 102, 30-48, doi:10.1016/j.atmosres.2011.07.009, 2011.

25 Chen, B., T., Fletcher, R., A., and Cheng, Y.,-S.: Calibration of Aerosol Instruments, in *Aerosol Measurement:*
26 *Principles, Techniques, and Applications*, Third Edition (eds P. Kulkarni, P. A. Baron and K. Willeke), John Wiley
27 & Sons, Inc., Hoboken, NJ, USA. doi:10.1002/9781118001684.ch21, 2011

28 Collins, D. R., Flagan, R. C., and Seinfeld, J. H.: Improved inversion of scanning DMA [Data](#)~~data~~, *Aerosol Sci.*
29 *Technol.*, 36:1, 1-9, doi:10.1080/027868202753339032, 2002.

30 Cornell, S. E.: Atmospheric nitrogen deposition: revising the question of the importance of the organic component,
31 *Environ. Pollut.*, 159, 2214–2222, doi:10.1016/j.envpol.2010.11.014, 2010.

1 DeCarlo, P. F., Slowik, J. G., Worsnop, D. R., Davidovits, P., and Jimenez, J. L.: Particle morphology and density
 2 characterization by combined mobility and aerodynamic diameter measurements. Part 1: Theory, *Aerosol Sci. Tech.*,
 3 38, 1185-1205, doi:10.1080/027868290903907, 2004.

4 ~~DeCarlo, P. F., Kimmel, J. R., Trimborn, A., Northway, M. J., Jayne, J. T., Aiken, A. C., Gonin, M., Fuhrer, K.,~~
 5 ~~Horvath, T., Docherty, K. S., Worsnop, D. R., and Jimenez, J. L.: Field-deployable, high-resolution, time-of-flight~~
 6 ~~aerosol-mass spectrometer, *Anal. Chem.*, 78, 8281-8289, doi:10.1021/ac061249n, 2006.~~

7 Drewnick, F., Schwab, J. J., Högrefe, O., Peters, S., Husain, L., Diamnon, D., Weber, R., and Demerjian, K. L.:
 8 Intercomparison and evaluation of four semi-continuous PM_{2.5} sulfate instruments, *Atmos. Environ.*, 37, 3335-3350,
 9 doi:10.1016/S1352-2310(03)00351-0, 2003.

10 Dunlea, E. J., Herndon, S. C., Nelson, D. D., Volkamer, R. M., San Martini, F., Sheehy, P. M., Zahniser, M. S.,
 11 Shorter, J. H., Wormhoudt, J. C., Lamb, B. K., Allwine, E. J., Gaffney, J. S., Marley, N. A., Grutter, M., Marquez,
 12 C., Blanco, S., Cardenas, B., Retama, A., Ramos Villegas, C. R., Kolb, C. E., Molina, L. T., and Molina, M. J.:
 13 Evaluation of nitrogen dioxide chemiluminescence monitors in a polluted urban environment, *Atmos. Chem. Phys.*,
 14 7, 2691-2704, doi:10.5194/acp-7-2691-2007, 2007.

15 Fahey, D., Eubank, C., Hübner, G., and Fehsenfeld, F.: Evaluation of a catalytic reduction technique for the
 16 measurement of total reactive odd-nitrogen NO_y in the atmosphere, *J. Atmos. Chem.*, 3, 435-468,
 17 doi:10.1007/BF00053871, 1985.

18 Fahey, D. W., Hübner, G., Parrish, D. D., Williams, E. J., Norton, R. B., Ridley, B. A., Singh, H. B., Liu, S. C., and
 19 Fehsenfeld, F. C.: Reactive nitrogen species in the troposphere: Measurements of NO, NO₂, HNO₃, particulate
 20 nitrate, peroxyacetyl nitrate (PAN), O₃, and total reactive odd nitrogen (NO_y) at Niwot Ridge, Colorado, *J. Geophys.*
 21 *Res.*, 91, 9781-9793, doi:10.1029/JD091iD09p09781, 1986.

22 Farmer, D. K., Matsunaga, A., Docherty, K. S., Surratt, J. D., Seinfeld, J. H., Ziemann, P. J., and Jimenez, J. L.:
 23 Response of an aerosol mass spectrometer to organonitrates and organosulfates and implications for atmospheric
 24 chemistry, *Proc. Natl. Acad. Sci. USA*, 107, 6670-6675, doi:10.1073/pnas.0912340107, 2010.

25 Forster, P., Ramaswamy, V., Artaxo, P., Bernsten, T., Betts, R., Fahey, D. W., Haywood, J., Lean, J., Lowe, D. C.,
 26 Myhre, G., Nganga, J., Prinn, R., Raga, G., Schulz, M., and Van Dorland, R.: Changes in Atmospheric Constituents
 27 and in Radiative Forcing, in: *Climate Change 2007: The Physical Science Basis. Contribution of Working Group I*
 28 *to the Fourth Assessment Report of the Intergovernmental Panel on Climate Change*, edited by: Solomon, S., Qin,
 29 D., Manning, M., Chen, Z., Marquis, M., Averyt, K. B., Tignor, M., and Miller, H. L., Cambridge University Press,
 30 Cambridge, United Kingdom and New York, NY, USA, 2007.

31 Froyd, K. D.: Ion induced nucleation in the atmosphere: Studies of ammonia, sulfuric acid, and water cluster ions,
 32 Ph.D., Department of Chemistry, University of Colorado, Boulder, Colorado, 282 pp., 2002.

1 Fuzzi, S., Baltensperger, U., Carslaw, K., Decesari, S., Denier van der Gon, H., Facchini, M. C., Fowler, D., Koren,
2 I., Langford, B., Lohmann, U., Nemitz, E., Pandis, S., Riipinen, I., Rudich, Y., Schaap, M., Slowik, J. G., Spracklen,
3 D. V., Vignati, E., Wild, M., Williams, M., and Gilardoni, S.: Particulate matter, air quality and climate: lessons
4 learned and future needs, *Atmos. Chem. Phys.*, 15, 8217–8299, doi:10.5194/acp-15-8217-2015, 2015.

5 Griffith, D. W. T., Mankin, W. G., Coffey, M. T., Ward, D. E., and Riebau, A.: FTIR remote sensing of biomass
6 burning emissions of CO₂, CO, CH₄, CH₂O, NO, NO₂, NH₃, and N₂O, in: *Global Biomass Burning: Atmospheric,*
7 *Climatic, and Biospheric Implications*, edited by: Levine, J. S., MIT Press, Cambridge, 230–239, 1991.

8 [Hallquist, M., Wenger, J. C., Baltensperger, U., Rudich, Y., Simpson, D., Claeys, M., Dommen, J., Donahue, N. M.,](#)
9 [George, C., Goldstein, A. H., Hamilton, J. F., Herrmann, H., Hoffmann, T., Iinuma, Y., Jang, M., Jenkin, M. E.,](#)
10 [Jimenez, J. L., Kiendler-Scharr, A., Maenhaut, W., McFiggans, G., Mentel, Th. F., Monod, A., Prévôt, A. S. H.,](#)
11 [Seinfeld, J. H., Surratt, J. D., Szmigielski, R., and Wildt, J.: The formation, properties and impact of secondary](#)
12 [organic aerosol: current and emerging issues, *Atmos. Chem. Phys.*, 9, 5155–5236, \[https://doi.org/10.5194/acp-9-\]\(https://doi.org/10.5194/acp-9-5155-2009\)](#)
13 [5155-2009, 2009.](#)

14 Hand, J. L., and S. M. Kreidenweis, A new method for retrieving particle refractive index and effective density from
15 aerosol size distribution data, *Aerosol Sci. Technol.*, 36, 1012 – 1026, doi:10.1080/02786820290092276, 2002.

16 Hardy, J. E. and Knarr, J. J.: Technique for measuring the total concentration of gaseous fixed nitrogen species, J.
17 *Air Pollut. Contr. Assoc.*, 32, 376–379, doi:10.1080/00022470.1982.10465412, 1982.

18 Hauglustaine, D. A., Balkanski, Y., and Schulz, M.: A global model simulation of present and future nitrate aerosols
19 and their direct radiative forcing of climate, *Atmos. Chem. Phys.*, 14, 11031–11063, doi:10.5194/acp-14-11031-
20 2014, 2014.

21 Haywood, J., Bush, M., Abel, S., Claxton, B., Coe, H., Crosier, J., Harrison, M., Macpherson, B., Naylor, M., and
22 Osborne, S.: Prediction of visibility and aerosol within the operational Met Office Unified Model II?: Validation of
23 model performance using observational data, *Q. J. Roy. Meteorol. Soc.*, 134, 1817–1832, doi:10.1002/qj.275, 2008.

24 Horstman, D. W.: A technique for measuring total oxides of nitrogen and ammonia by chemiluminescent detection,
25 *Analysis Instr.*, 93–98, 1982.

26 Hu, D., Chen, J., Ye, X., and Yang, X.: Hygroscopicity and evaporation of ammonium chloride and ammonium
27 nitrate: Relative humidity and size effects on the growth factor, *Atmos. Environ.*, 45, 2349–2355,
28 doi:10.1016/j.atmosenv.2011.02.024, 2011.

29 Huffman, J. A., Docherty, K. S., Aiken, A. C., Cubison, M. J., Ulbrich, I. M., DeCarlo, P. F., Sueper, D., Jayne, J.
30 T., Worsnop, D. R., Ziemann, P. J., and Jimenez, J. L.: Chemically-resolved aerosol volatility measurements from
31 two megacity field studies, *Atmos. Chem. Phys.*, 9, 7161–7182, doi:10.5194/acp-9-7161-2009, 2009.

32 IPCC: Climate Change 2013, The Physical Science Basis, Bern, Switzerland, 2013.

1 Jayne, J. T., Leard, D. C., Zhan, X., Davidovits, P., Smith, K. A., Kolb, C. E., and Worsnop, D. R.: Development of
2 an aerosol mass spectrometer for size and composition analysis of submicron particles, *Aerosol Sci. and Technol.*,
3 33:1-2, 49-70, doi: 10.1080/027868200410840, 2000.

4 Jimenez, J. L., Canagaratna, M. R., Donahue, N. M., Prevot, A. S. H., Zhang, Q., Kroll, J. H., DeCarlo, P. F., Allan,
5 J. D., Coe, H., Ng, N. L., Aiken, A. C., Docherty, K. S., Ulbrich, I. M., Grieshop, A. P., Robinson, A. L., Duplissy,
6 J., Smith, J. D., Wilson, K. R., Lanz, V. A., Hueglin, C., Sun, Y. L., Tian, J., Laaksonen, A., Raatikainen, T.,
7 Rautiainen, J., Vaattovaara, P., Ehn, M., Kulmala, M., Tomlinson, J. M., Collins, D. R., Cubison, M. J., Dunlea, E.
8 J., Huffman, J. A., Onasch, T. B., Alfarra, M. R., Williams, P. I., Bower, K., Kondo, Y., Schneider, J., Drewnick, F.,
9 Borrmann, S., Weimer, S., Demerjian, K., Salcedo, D., Cottrell, L., Griffin, R., Takami, A., Miyoshi, T.,
10 Hatakeyama, S., Shimono, A., Sun, J. Y., Zhang, Y. M., Dzepina, K., Kimmel, J. R., Sueper, D., Jayne, J. T.,
11 Herndon, S. C., Trimborn, A. M., Williams, L. R., Wood, E. C., Middlebrook, A. M., Kolb, C. E., Baltensperger, U.,
12 and Worsnop, D. R.: Evolution of organic aerosols in the atmosphere, *Science*, 326, 1525–1529,
13 doi:10.1126/science.1180353, 2009.

14 Jimenez, J. L., Canagaratna, M. R., Drewnick, F., Allan, J. D., Alfarra, M. R., Middlebrook, A. M., Slowik, J. G.,
15 Zhang, Q., Coe, H., Jayne, J. T., and Worsnop, D. R.: Comment on “The effects of molecular weight and thermal
16 decomposition on the sensitivity of a thermal desorption aerosol mass spectrometer”, *Aerosol Sci. and Technol.*,
17 50(9), i-xv, 2016.

18 Jickells, T., Baker, A., R., Cape, J., N., Cornell, S., E., and Nemitz, E.: The cycling of organic nitrogen through the
19 atmosphere, *Philos. Trans. R Soc. Lond. B Biol. Sci.*, 368, 1621, doi: 10.1098/rstb.2013.0115, 2013.

20 Kamal, M. S., Razzak, S. A., and Hossain, M. M.: Catalytic oxidation of volatile organic compounds (VOCs) - A
21 review, *Atmos. Environ.*, 140, 117-134, doi:10.1016/j.atmosenv.2016.05.031, 2016

22 Kiyoura, R. and Urano, K.: Mechanism, kinetics and equilibrium of thermal decomposition of ammonium sulfate,
23 *Ind. Eng. Chem. Process Des. Develop.*, 9, 489-494, doi:10.1021/i260036a001, 1970.

24 Knutson, E. O. and Whitby, K. T.: Aerosol classification by electric mobility: Apparatus, theory, and applications, *J.*
25 *Aerosol Sci.*, 6, 443–451, doi:10.1016/0021-8502(75)90060-9, 1975.

26 [Koss, A. R., Sekimoto, K., Gilman, J. B., Selimovic, V., Coggon, M. M., Zarzana, K. J., Yuan, B., Lerner, B. M.,](#)
27 [Brown, S. S., Jimenez, J. L., Krechmer, J., Roberts, J. M., Warneke, C., Yokelson, R. J., and de Gouw, J.: Non-](#)
28 [methane organic gas emissions from biomass burning: identification, quantification, and emission factors from PTR-](#)
29 [ToF during the FIREX 2016 laboratory experiment, *Atmos. Chem. Phys.*, 18, 3299-3319,](#)
30 <https://doi.org/10.5194/acp-18-3299-2018>, 2018.

31 [Koss, A. R., Sekimoto, K., Gilman, J. B., Selimovic, V., Coggon,](#)
32 [M. M., Zarzana, K. J., Yuan, B., Lerner, B. M., Brown, S. S., Jimenez, J. L., Krechmer, J., Roberts, J. M., Warneke,](#)
33 [C., Yokelson, R. J., and de Gouw, J.: Non-methane organic gas emissions from biomass burning: identification,](#)

1 [quantification, and emission factors from PTR-ToF during the FIREX 2016 laboratory experiment, Atmos. Chem.](#)
2 [Phys. Discuss., <https://doi.org/10.5194/acp-2017-924>, in review, 2017.](#)

3 Kostianinen, R., and Kaupila, T. J.: Effect of eluent on the ionization process in liquid chromatography-mass
4 spectrometry, *J. Chrom. A.*, 1216(4), 685-699, doi:10.1016/j.chroma.2008.08.095, 2009.

5 Kuhlbusch, T. A., Lobert, J. M., Crutzen, P. J., and Warneck, P.: Molecular nitrogen emissions from denitrification
6 during biomass burning, *Nature*, 351, 135-137, doi:10.1038/351135a0, 1991.

7 [Kupc, A., Williamson, C., Wagner, N. L., Richardson, M., and Brock, C. A.: Modification, calibration, and](#)
8 [performance of the Ultra-High Sensitivity Aerosol Spectrometer for particle size distribution and volatility](#)
9 [measurements during the Atmospheric Tomography Mission \(ATom\) airborne campaign, Atmos. Meas. Tech., 11,](#)
10 [369-383, <https://doi.org/10.5194/amt-11-369-2018>, 2018.](#)~~[Kupe, A., Williamson, C., Wagner, N. L., Richardson, M.,](#)~~
11 ~~[and Brock, C. A.: Modification, Calibration, and Performance of the Ultra-High Sensitivity Aerosol Spectrometer](#)~~
12 ~~[for Particle Size Distribution and Volatility Measurements During the Atmospheric Tomography \(ATom\) Airborne](#)~~
13 ~~[Campaign, Atmos. Meas. Tech. Discuss., <https://doi.org/10.5194/amt-2017-293>, in review, 2017.](#)~~

14 Lee, B. H., Mohr, C., Lopez-Hilfiker, F. D., Lutz, A., Hallquist, M., Lee, L., Romer, P., Cohen, R. C., Iyer, S.,
15 Kurten, T., Hu, W. W., Day, D. A., Campuzano-Jost, P., Jimenez, J. L., Xu, L., Ng, N. L., Guo, H., Weber, R. J.,
16 Wild, R. J., Brown, S. S., Koss, A., de Gouw, J., Olson, K., Goldstein, A. H., Seco, R., Kim, S., McAvey, K. M.,
17 Shepson, P. B., Starn, T., Baumann, K., Edgerton, E., Liu, J., Shilling, J. E., Miller, D. O., Brune, W. H.,
18 Schobesberger, S., D'Ambro, E. L., and Thornton, J. A.: Highly functionalized organic nitrates in the Southeast
19 U.S.: contribution to secondary organic aerosol and reactive nitrogen budgets, *Proc. Natl. Acad. Sci.*, 113, 1516–
20 1521, doi:10.1073/pnas.1508108113, 2016.

21 Li, J., Wang, W.-C., Liao, H., and Chang, W.: Past and future direct radiative forcing of nitrate aerosol in East Asia,
22 *Theor. Appl. Climatol.*, 121, 445-458, doi: 10.1007/s00704-014-1249-1, 2015.

23 Liao, H., Adams, P. J., Chung, S. H., Seinfeld, J. H., Mickley, L. J., and Jacob, D. J.: Interactions between
24 tropospheric chemistry and aerosols in a unified general circulation model, *J. Geophys. Res.*, 108(D1), 4001,
25 doi:10.1029/2001JD001260, 2003.

26 Lin, M., Walker, J., Geron, C., and Khlystov, A.: Organic nitrogen in PM_{2.5} aerosol at a forest site in the Southeast
27 US, *Atmos. Chem. Phys.*, 10, 2145-2157, doi:10.5194/acp-10-2145-2010, 2010.

28 Liu, Y., and Daum, P. H.: The effect of refractive index on size distributions and light scattering coefficients derived
29 from optical particle counters, *J. Aerosol Sci.*, 31, 945-957, doi:10.1016/S0021-8502(99)00573-X, 2000.

30 Liu, B. Y. H. and Lee, K.W.: An aerosol generator of high stability, *Am. Ind. Hyg. Assoc. J.*, 36, 861–865,
31 doi:10.1080/0002889758507357, 1975.

1 Lobert, J. M., Scharffe, D. H., Hao, W. M., and Crutzen, P. J.: Importance of biomass burning in the atmospheric
2 budgets of nitrogen-containing gases, *Nature*, 346, 552-554, doi:10.1038/346552a0, 1990.

3 Lobert, J. M., Scharffe, D. H., Hao, W.-M., Kuhlbusch, T. A., Seuwen, R., Warneck, P., and Crutzen, P. J.:
4 Experimental evaluation of biomass burning emissions: Nitrogen and carbon containing compounds. In: *Global*
5 *Biomass Burning: Atmospheric, Climatic, and Biospheric Implications*, Levine, J. S. (Ed.), The MIT Press,
6 Cambridge, MA, 1991.

7 [Lovejoy, E. R.: Ion trap studies of \$H_3^+\(H_2SO_4\)_m\(H_2O\)_n\$ reactions with water, ammonia, and a variety of organic](#)
8 [compounds, *Int. J. Mass Spectrom.*, 190/191, 231-241, 1999.](#)

9 Ma, Y.: Developments and Improvements to the Particle-Into-Liquid Sampler (PILS) and its Application to Asian
10 Outflow Studies, Ph.D. Dissertation, Georgia Institute of Technology, Atlanta, GA, 2004.

11 Maris, C., Chung, M. Y., Lueb, R., Krischke, U., Meller, R., Fox, M. J., and Paulson, S. E.: Development of
12 instrumentation for simultaneous analysis of total non-methane organic carbon and volatile organic compounds in
13 ambient air, *Atmos. Environ.*, 37, S149-S158, doi:10.1016/S1352-2310(03)00387-X, 2003.

14 Marx, O., Brümmner, C., Ammann, C., Wolff, V., and Freibauer, A.: TRANC – a novel fast-response converter to
15 measure total reactive atmospheric nitrogen, *Atmos. Meas. Tech.*, 5, 1045-1057, doi:10.5194/amt-5-1045-2012,
16 2012.

17 McCalley, C. K. and Sparks, J. P.: Abiotic gas formation drives nitrogen loss from a desert ecosystem, *Science*, 326,
18 837–840, doi:10.1126/science.1178984, 2009.

19 McMeeking, G. R., Kreidenweis, S. M., Baker, S., Carrico, C. M., Chow, J. C., Collet Jr., J. L., Hao, W. M.,
20 Holden, A. S., Kirchstetter, T. W., Malm, W. C., Moosmüller, H., Sullivan, A. P., and Wold, C. E.: Emissions of
21 trace gases and aerosols during the open combustion of biomass in the laboratory, *J. Geophys. Res.*, 114, D19210,
22 doi:10.1029/2009JD011836, 2009.

23 McMurry, P. H.: A review of atmospheric aerosol measurements, *Atmos. Environ.*, 34, 1959-1999,
24 doi.org/10.1016/S1352-2310(99)00455-0, 2000.

25 Min, K.-E., Washenfelder, R. A., Dubé, W. P., Langford, A. O., Edwards, P. M., Zarzana, K. J., Stutz, J., Lu, K.,
26 Rohrer, F., Zhang, Y., and Brown, S. S.: A broadband cavity enhanced absorption spectrometer for aircraft
27 measurements of glyoxal, methylglyoxal, nitrous acid, nitrogen dioxide, and water vapor, *Atmos. Meas. Tech.*, 9,
28 423-440, <https://doi.org/10.5194/amt-9-423-2016>, 2016.

29 Murphy, D. M.: The effects of molecular weight and thermal decomposition on the sensitivity of a thermal
30 desorption aerosol mass spectrometer, *Aerosol Sci. and Technol.*, 50(2), 118-125,
31 doi:10.1080/02786826.2015.1136403, 2016a.

Formatted: Superscript

Formatted: Subscript

Formatted: Subscript

Formatted: Subscript

Formatted: Subscript

Formatted: Subscript

1 Murphy, D. M.: Reply to Comment on the effects of molecular weight and thermal decomposition on the sensitivity
2 of a thermal desorption aerosol mass spectrometer”, by Jimenez et al., *Aerosol Sci. and Technol.*, 50, 1277-1283,
3 2016b.

4 Neff, J. C., Holland, E. A., Dentener, F. J., McDowell, W. H., and Russell, K. M.: The origin, composition and rates
5 of organic nitrogen deposition: A missing piece of the nitrogen cycle?, *Biogeochemistry*, 57, 99–136, 2002.

6 Neuman, J. A., Huey, L. G., Ryerson, T. B., and Fahey, D. W.: Study of inlet materials for sampling atmospheric
7 nitric acid, *Environ. Sci. Technol.*, 33(7), 1133-1136, doi: 10.1021/es980767f, 1999.

8 Neuman, J. A., Ryerson, T. B., Huey, L. G., Jakoubek, R., Nowak, J. B., Simons, G., and Fehsenfeld, F. C.:
9 Calibration and evaluation of nitric acid and ammonia permeation tubes by UV optical absorption, *Environ. Sci.*
10 *Technol.*, 37, 2975-2981, doi:10.1021/es026422l, 2003.

11 NIST Chemical Kinetics Database, Standard Reference Database 17, Version 7.0 Web Version, accessed September
12 18, 2017.

13 Orsini, D. A., Ma, Y., Sullivan, A., Sierau, B., Baumann, K., and Weber, R. J.: Refinements to the particle-into-
14 liquid sampler (PILS) for ground and airborne measurements of water-soluble aerosol composition, *Atmos.*
15 *Environ.*, 37, 1243–1259, doi:10.1016/S1352-2310(02)01015-4, 2003.

16 Park, R. S., Lee, S., Shin, S.-K., and Song, C. H.: Contribution of ammonium nitrate to aerosol optical depth and
17 direct radiative forcing by aerosols over East Asia, *Atmos. Chem. Phys.*, 14, 2185-2201, doi:10.5194/acp-14-2185-
18 2014, 2014.

19 Parrish, D. D. and Fehsenfeld, F. C.: Methods for gas-phase measurements of ozone, ozone precursors and aerosol
20 precursors, *Atmos. Environ.*, 34, 1921–1957, doi: 10.1016/S1352-2310(99)00454-9, 2000.

21 Pöschl, U.: Atmospheric aerosols: Composition, transformation, climate and health effects, *Angew. Chem. Int. Ed.*,
22 44, 7520-7540, doi:10.1002/anie.200501122, 2005.

23 Prenni, A. J., Levin, E. J. T., Benedict, K. B., Sullivan, A. P., Schurman, M. I., Gebhart, K. A., Day, D. E., Carrico,
24 C. M., Malm, W. C., Schichtel, B. A., Collet Jr., J. L., and Kreidenweis, S. M.: Gas-phase reactive nitrogen near
25 Grand Teton National Park: Impacts of transport, anthropogenic emissions, and biomass burning, *Atmos. Environ.*,
26 89, 749-756, doi:10.1016/j.atmosenv.2014.03.017, 2014.

27 Roberts, J. M., Bertman, S. B., Jobson, T., Niki, H., and Tanner, R.: Measurement of total nonmethane organic
28 carbon (Cy): development and application at Chebogue Point, Nova Scotia, during the 1993 North Atlantic Regional
29 Experiment campaign, *J. Geophys. Res.-Atmos.*, 103, 13581–13592, doi:10.1029/97JD02240, 1998.

30 Roberts, J. M., Veres, P., Warneke, C., Neuman, J. A., Washenfelder, R. A., Brown, S. S., Baasandorj, M.,
31 Burkholder, J. B., Burling, I. R., Johnson, T. J., Yokelson, R. J., and de Gouw, J.: Measurement of HONO, HNCO,

1 and other inorganic acids by negative-ion proton-transfer chemical-ionization mass spectrometry (NI-PT-CIMS):
2 application to biomass burning emissions, *Atmos. Meas. Tech.*, 3, 981-990, doi:10.5194/amt-3-981-2010, 2010.

3 Rosenberg, P. D., Dean, A. R., Williams, P. I., Dorsey, J. R., Minikin, A., Pickering, M. A., and Petzold, A.: Particle
4 sizing calibration with refractive index correction for light scattering optical particle counters and impacts upon
5 PCASP and CDP data collected during the Fennec campaign, *Atmos. Meas. Tech.*, 5, 1147-1163, doi:10.5194/amt-
6 5-1147-2012, 2012.

7 Russell, L. M., Flagan, R. C., and Seinfeld, J. H.: Asymmetric instrument response resulting from mixing effects in
8 accelerated DMA-CPC measurements, *Aerosol Sci. Technol.*, 23:4, 491-509, doi: 10.1080/02786829508965332,
9 1995.

10 Saylor, R. D., Edgerton, E. S., Hartsell, B. E., Baumann, K., and Hansen, D. A.: Continuous gaseous and total
11 ammonia measurements from the southeastern aerosol research and characterization (SEARCH) study, *Atmos.*
12 *Environ.*, 44, 4994-5004, doi:10.1016/j.atmosenv.2010.07.055, 2010.

13 Schwab, J. J., Li, Y., Bae, M.-S., Demerjian, K. L., Hou, J., Zhou, X., Jensen, B., and Pryor, S.: A laboratory
14 intercomparison of real-time gaseous ammonia measurement methods, *Environ. Sci. Technol.*, 41, 8412-8419,
15 doi:10.1021/es070354r, 2007.

16 Schwartz, A., Holbrook, L. L., and Wise, H.: Catalytic oxidation studies with platinum and palladium, *J. Catalysis*,
17 21, 199-207, doi: 10.1016/0021-9517(71)90138-2, 1971.

18 [Selimovic, V., Yokelson, R. J., Warneke, C., Roberts, J. M., de Gouw, J., Reardon, J., and Griffith, D. W. T.:
19 *Aerosol optical properties and trace gas emissions by PAX and OP-FTIR for laboratory-simulated western US
20 wildfires during FIREX*, *Atmos. Chem. Phys.*, 18, 2929-2948, <https://doi.org/10.5194/acp-18-2929-2018>,
21 2018.](#)
22 ~~[Selimovic, V., Yokelson, R. J., Warneke, C., Roberts, J. M., de Gouw, J., Reardon, J., and Griffith, D. W. T.:
23 *Aerosol optical properties and trace gas emissions by PAX and OP-FTIR for laboratory-simulated western US
24 wildfires during FIREX*, *Atmos. Chem. Phys. Discuss.*, <https://doi.org/10.5194/acp-2017-859>, in review, 2017.](#)~~

24 Sorooshian, A., Brechtel, F. J., Ma, Y., Weber, R. J., Corless, A., Flagan, R. C., and Seinfeld, J. H.: Modeling and
25 characterization of a Particle-into-Liquid Sampler (PILS), *Aerosol Sci. Tech.*, 40,396-409,
26 doi:10.1080/02786820600632282, 2006.

27 Stockwell, C. E., Yokelson, R. J., Kreidenweis, S. M., Robinson, A. L., DeMott, P. J., Sullivan, R. C., Reardon, J.,
28 Ryan, K. C., Griffith, D. W. T., and Stevens, L.: Trace gas emissions from combustion of peat, crop residue,
29 domestic biofuels, grasses, and other fuels: configuration and Fourier transform infrared (FTIR) component of the
30 fourth Fire Lab at Missoula Experiment (FLAME-4), *Atmos. Chem. Phys.*, 14, 9727-9754, doi:10.5194/acp-14-
31 9727-2014, 2014.

1 Stockwell, C. E., Veres, P. R., Williams, J., and Yokelson, R. J.: Characterization of biomass burning emissions
2 from cooking fires, peat, crop residue, and other fuels with high-resolution proton-transfer-reaction time-of-flight
3 mass spectrometry, *Atmos. Chem. Phys.*, 15, 845-865, doi:10.5194/acp-15-845-2015, 2015.

4 Stolzenburg, M.: An Ultrafine Aerosol Size Distribution Measuring System, PhD. thesis, Mechanical Engineering
5 Department, University of Minnesota, USA, 1988.

6 Stolzenburg, M. R., and McMurry, P. H.: An ultrafine aerosol condensation nucleus counter, *Aerosol Sci. Technol.*,
7 14(1), 48-65, doi:10.1080/02786829108959470, 1991.

8 Takegawa, N., Miyazaki, Y., Kondo, Y., Komazaki, Y., Miyakawa, T., Jimenez, J. L., Jayne, J. T., Worsnop, D. R.,
9 Allan, J. D., and Weber, R. J.: Characterization of an Aerodyne aerosol mass spectrometer (AMS): Intercomparison
10 with other aerosol instruments, *Aerosol Sci. Technol.*, 39 (8), 760-770, doi:10.1080/02786820500243404, 2005.

11 Tang, K., Page, J. S., and Smith, R. D.: Charge competition and the linear dynamic range of detection in
12 electrospray ionization mass spectrometry, *J. Am. Soc. Mass Spectrom.*, 15, 1416-1423,
13 doi:10.1016/j.jasms.2004.04.034, 2004.

14 [Tannenbaum, E., Coffin, E. M., and Harrison, A. J.: The far ultraviolet absorption spectra of simple alkyl amines, *J.*
15 *Chem. Phys.*, 21, 311, doi: <https://doi.org/10.1063/1.1698878>, 1953.](https://doi.org/10.1063/1.1698878)

16 Usherenko, L. N., Fialko, M. B., Kumok, V. N., and Skorik, A. I.: Mechanism and kinetics of thermal-
17 decomposition of ammonium oxalate, *J. Appl. Chem. USSR*, 61, 1559-1563, 1988.

18 Valentour, J. C., Aggarwal, V., and Sunshine, I.: Sensitive gas chromatographic determination of cyanide, *Anal.*
19 *Chem.*, 46 (7), 924-925, doi:10.1021/ac60343a048, 1974.

20 Veres, P. V., Roberts, J. M., Warneke, C., and deGouw, J.: Development of negative-ion proton-transfer chemical-
21 ionization mass spectrometry (NI-PT-CIMS) for the measurement of gas-phase organic acids in the atmosphere, *Int.*
22 *J. Mass Spectrom.*, 274(1-3), 48-55, doi:10.1016/j.ijms.2008.04.032, 2008.

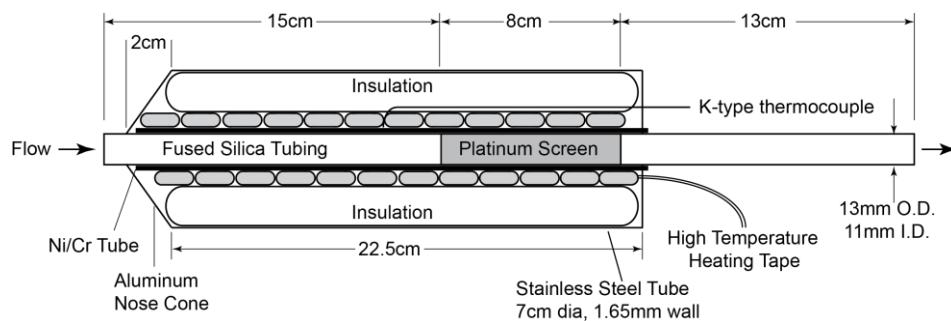
23 Veres, P., Gilman, J. B., Roberts, J. M., Kuster, W. C., Warneke, C., Burling, I. R., and de Gouw, J.: Development
24 and validation of a portable gas phase standard generation and calibration system for volatile organic compounds,
25 *Atmos. Meas. Tech.*, 3, 683-691, doi:10.5194/amt-3-683-2010, 2010.

26 Vieno, M., Heal, M. R., Twigg, M. M., MacKenzie, I. A., Braban, C. F., Lingard, J. J. N. Ritchie, S., Beck, R. C.,
27 A., M., Ots, R., DiMarco, C. F., Nemitz, E., Sutton, M. A., and Reis, S.: The UK particulate matter air pollution
28 episode of March-April 2014: more than Saharan dust., *Environ. Res. Lett.*, doi:10.1088/1748-9326/11/4/044004,
29 2016.

30 Wang, S. C., and Flagan, R. C.: Scanning electrical mobility spectrometer, *Aerosol Sci. Technol.*, 13, 230-240,
31 doi:10.1080/02786829008959441, 1990.

- 1 Weber, R. J., Orsini, D., Daun, Y., Lee, Y. N., Klotz, P. J., and Brechtel, F. J.: A [Particleparticle-Into-Liquid](#)
2 [liquid Collector-collector](#) for [Rapid-rapid Measurement-measurement](#) of [Aerosol-aerosol Bulk-bulk Chemical](#)
3 [chemical Compositioncomposition](#), Aerosol Sci. Technol. 35, 718–727, doi:10.1080/02786820152546761, 2001.
- 4 Wiedensohler, A.: An approximation of the bipolar charge distribution for particles in the sub-micron size range, J.
5 Aerosol Sci., 19, 387–389, doi:10.1016/0021-8502(88)90278-9, 1988.
- 6 Williams, E. J., Baumann, K., Roberts, J. M., Bertman, S. B., Norton, R. B., Fehsenfeld, F. C., Springston, S. R.,
7 Nunnermacker, L. J., Newman, L., Olszyna, K., Meagher, J., Hartsell, B., Edgerton, E., Pearson, J. R., and Rodgers,
8 M. O.: Intercomparison of ground-based NOy measurement techniques, J. Geophys. Res.-Atmos., 103, 22261-
9 22280, doi:10.1029/98JD00074, 1998.
- 10 Winer, A. M., Peters, J. W., Smith, J. P., and Pitts, J. N.: Response of commercial chemiluminescent nitric oxide-
11 nitrogen dioxide analyzers to other nitrogen-containing compounds, Environ. Sci. Technol., 8, 1118-1121,
12 doi:10.1021/es60098a004, 1974.
- 13 Womack, C. C., Neuman, J. A., Veres, P. R., Eilerman, S. J., Brock, C. A., Decker, Z. C. J., Zarzana, K. J., Dube,
14 W. P., Wild, R. J., Wooldridge, P. J., Cohen, R. C., and Brown, S. S.: Evaluation of the accuracy of thermal
15 dissociation CRDS and LIF techniques for atmospheric measurement of reactive nitrogen species, Atmos. Meas.
16 Tech., 10, 1911-1926, doi:10.5194/amt-10-1911-2017, 2017.
- 17 Xu, L. and Penner, J. E.: Global simulations of nitrate and ammonium aerosols and their radiative effects, Atmos.
18 Chem. Phys., 12, 9479-9504, doi:10.5194/acp-12-9479-2012, 2012.
- 19 [Yokelson, R. J., Griffith, D. W. T., and Ward, D. E.: Open path Fourier transform infrared studies of large-scale](#)
20 [laboratory biomass fires, J. Geophys. Res., 101, 21067–21080, doi:10.1029/96jd01800, 1996.](#)
- 21 Yokelson, R. J., Christian, T. J., Bertschi, I. T., and Hao, W. M.: Evaluation of adsorption effects on measurements
22 of ammonia, acetic acid, and methanol, J. Geophys. Res., 108, 4649, doi:10.1029/2003JD003549, 2003.

1 **Figures**



2
3 **Figure 1.** Diagram of the custom-built platinum catalyst system for the total reactive nitrogen instrument (N_T) operated
4 at 750°C. The outlet flow is followed by a molybdenum oxide catalyst before the ~~commercial~~-custom NO-O₃
5 chemiluminescent instrument.

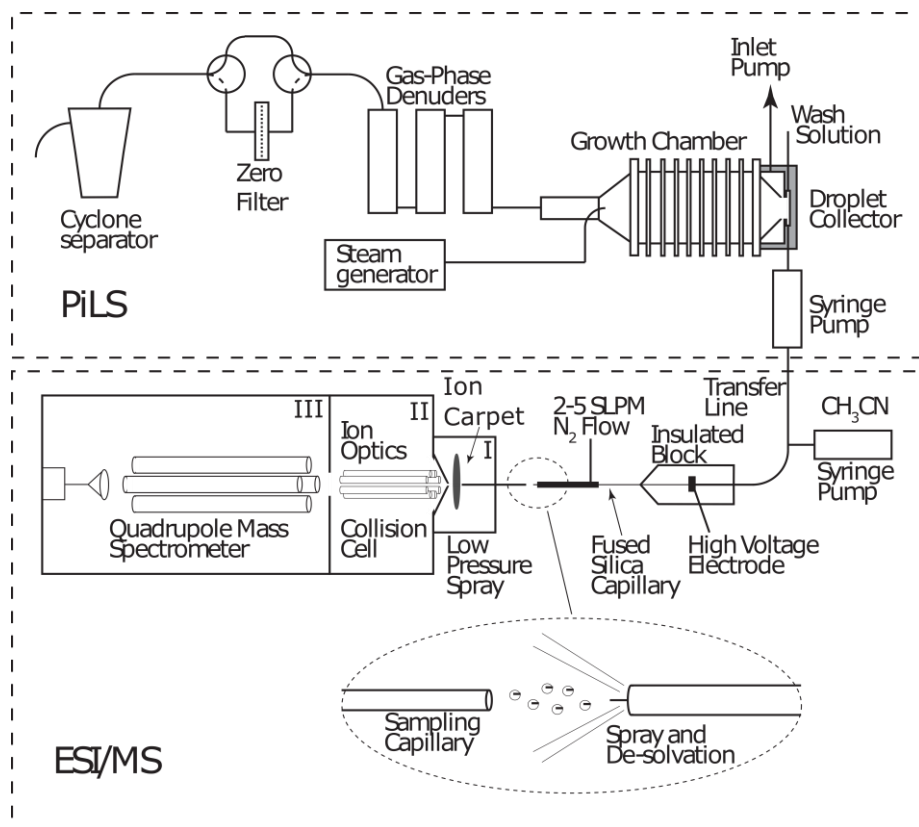


Figure 2. Schematic of a particle-into-liquid sampler (PILS; Sorooshian et al., 2006) interfaced to an electrospray ionization (ESI) source of a quadrupole mass spectrometer (MS) for continuous measurement of water soluble components of atmospheric particles.

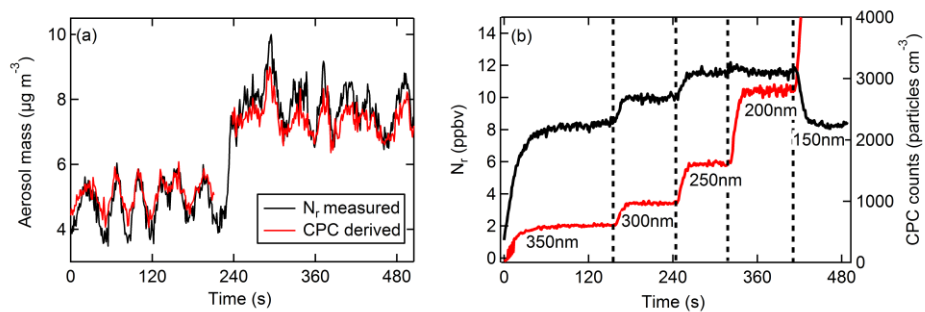


Figure 3. The signal resulting from particles only. (a) Real-time N_r (black) measured and CPC (red) derived aerosol mass concentrations ($\mu\text{g m}^{-3}$) from an atomized solution of NaNO_3 . (b) Time response of the N_r signal (ppbv) shown in black (left axis), and the CPC signal (particles cm^{-3}), shown in red (right axis), as particle sizes of $(\text{NH}_4)_2\text{SO}_4$ are selectively changed. The dashed vertical lines and labels indicate the singly-charged particle diameter selected with the DMA.

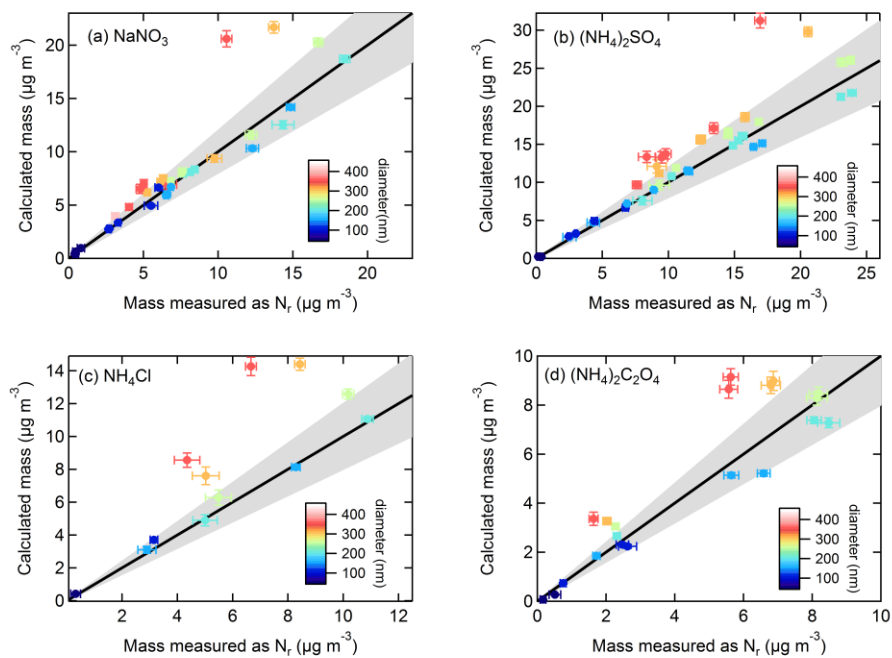


Figure 4. Calculated mass from particles size-selected by the DMA and corrected for multiply charged particles using SMPS-derived size distributions compared to aerosol mass concentrations ($\mu\text{g m}^{-3}$) measured as N_r for (a) NaNO_3 , (b) $(\text{NH}_4)_2\text{SO}_4$, (c) NH_4Cl , and (d) $(\text{NH}_4)_2\text{C}_2\text{O}_4$. The particle size is designated by the color plot (error bars indicate ± 1 stdev) and the 1:1 line is shown in black with 20% error indicated by the grey shading.

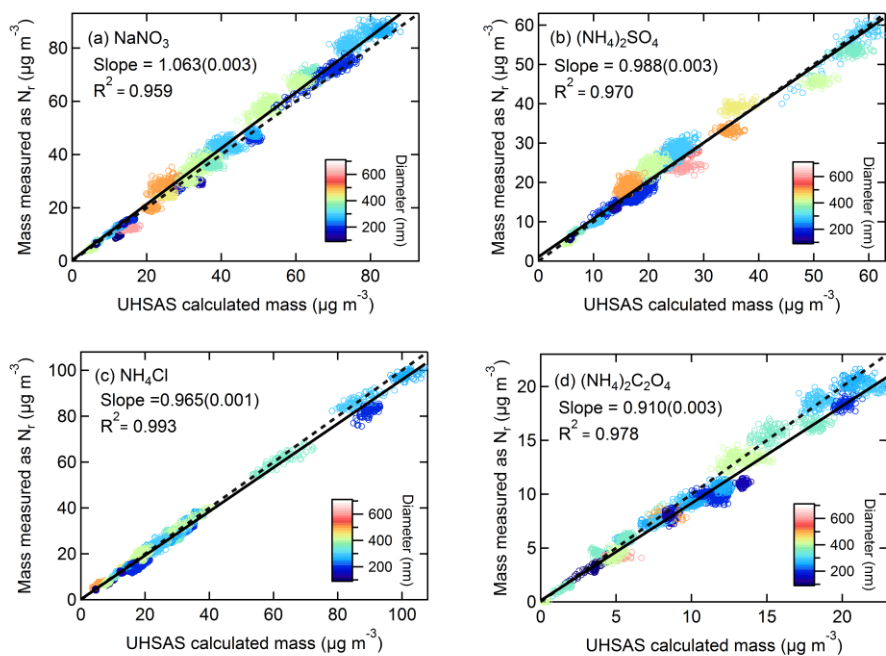


Figure 5. Correlation plots of mass concentrations measured as N_r for (a) NaNO_3 , (b) $(\text{NH}_4)_2\text{SO}_4$, (c) NH_4Cl , and (d) $(\text{NH}_4)_2\text{C}_2\text{O}_4$ versus mass concentrations calculated using CPC number concentrations with UHSAS size distributions. Particle sizes (nm) are indicated by the color plot and the 1:1 line is shown in dashed black. The solid lines are orthogonal distance regression fits. The slope (uncertainty) and R^2 is shown.

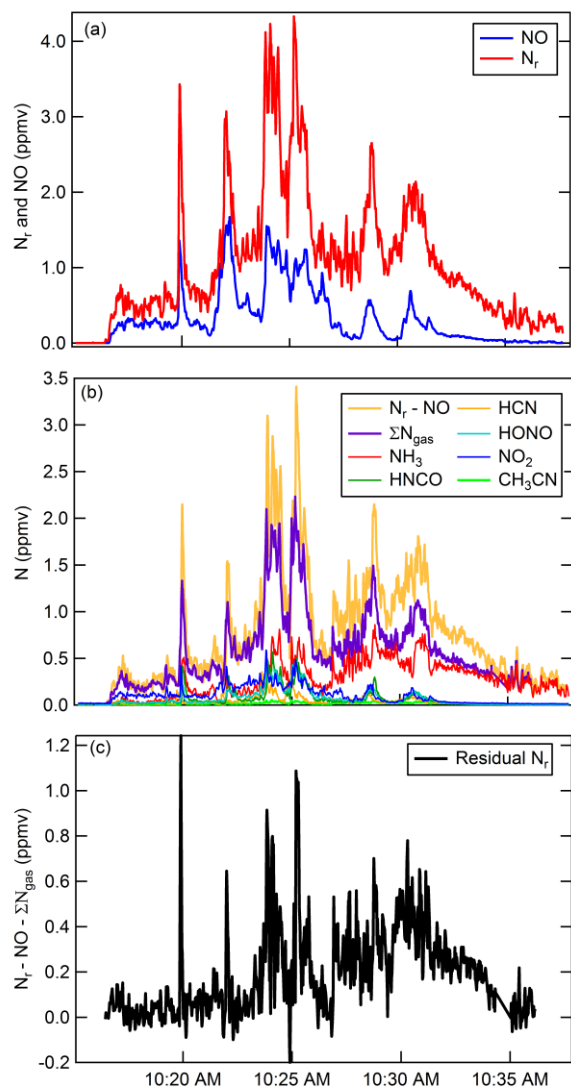


Figure 6. Timeseries for Fire Sciences Lab 2016 measurements of emissions from a subalpine fir canopy sample (Fire 047). (a) Total reactive nitrogen (N_r , red) and nitric oxide (NO, blue) measurements. (b) Comparison of the difference ($N_r - NO$, gold) with the sum of the measured gas phase N_r species (purple). The sum of individually measured gas-phase species in order of abundance include: NH_3 , $HNCO$, HCN , $HONO$, NO_2 , CH_3NO_2 , and 40 minor organic nitrogen species. NO_2 and $HONO$ were measured by a broadband-cavity enhanced extinction spectrometer, HCN and NH_3 were measured by FTIR, and all remaining organic species were measured by H_2O^+ CIMS. (c) Residual N_r in ppmv.

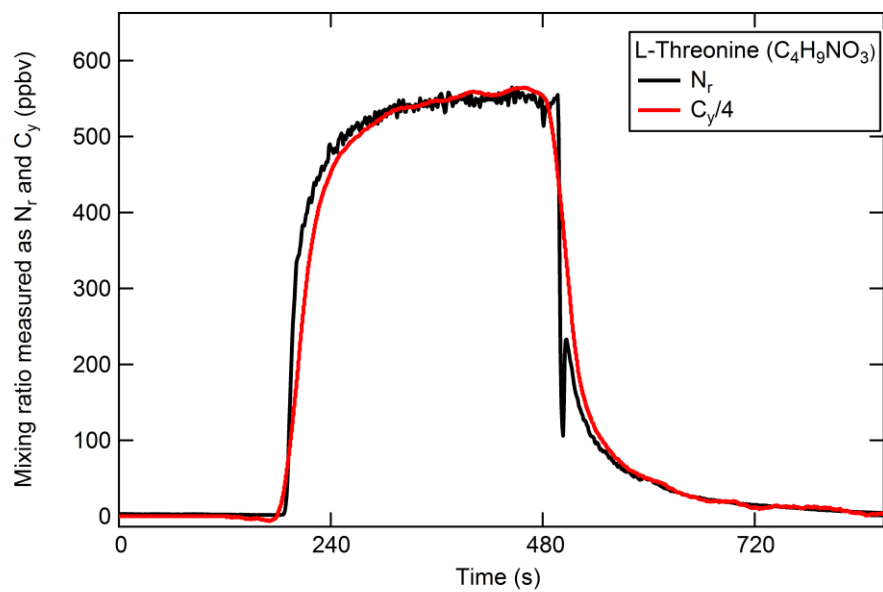


Figure 76. An example of the quantitative conversion of atomized polydisperse threonine ($C_4H_9NO_3$) to NO and CO₂ measured by NO-O₃ chemiluminescence and a LICOR-6251, respectively. The measured total C_y (red) is divided by

| *the number of C atoms in threonine (4).*

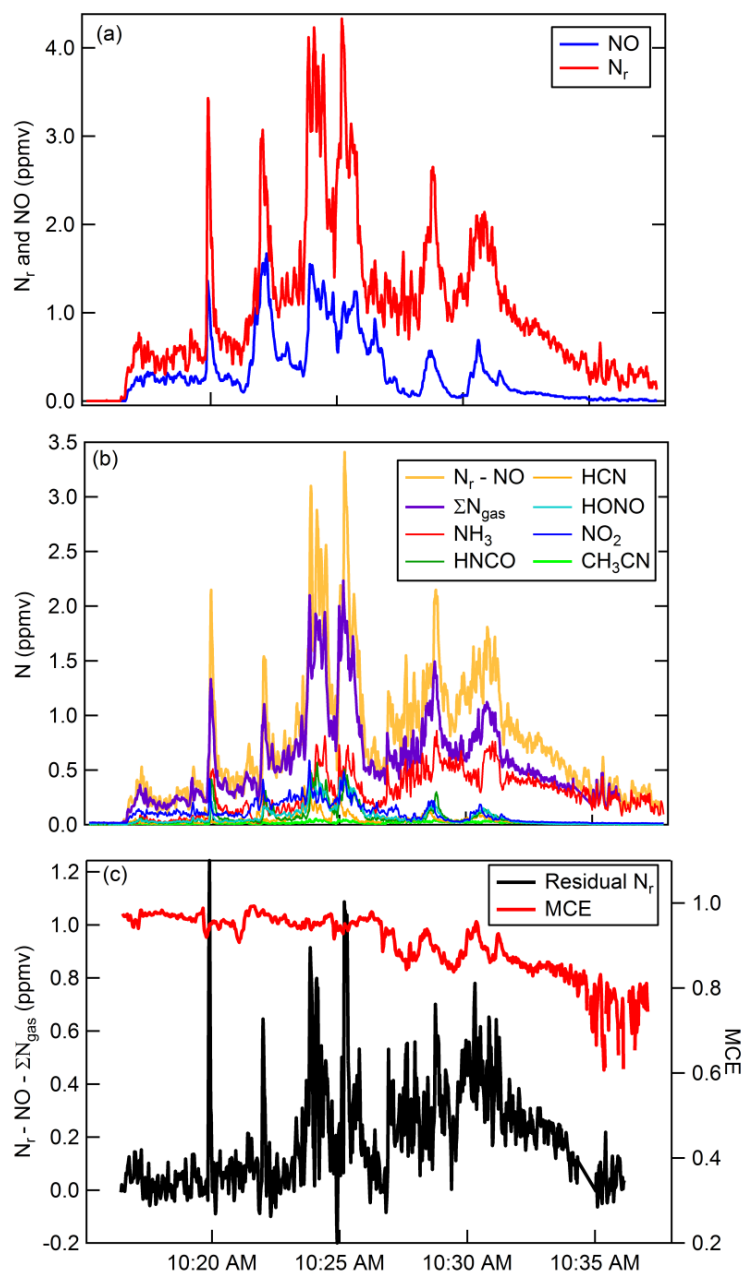


Figure 7. Timeseries for Fire Sciences Lab 2016 measurements of emissions from a subalpine fir canopy sample (Fire 047). (a) Total reactive nitrogen (N_r , red) and nitric oxide (NO, blue) measurements. (b) Comparison of the difference (N_r -NO, gold) with the sum of the measured gas phase N_r -species (purple). The sum of individually measured gas-phase species in order of abundance include: NH_3 , HNCO, HCN, HONO, NO_2 , CH_3NO_2 , and 40 minor organic nitrogen species. NO_2 and HONO were measured by a broadband cavity enhanced extinction spectrometer, HCN and NH_3 were measured by FTIR, and all remaining organic species were measured by H_3O^+ CIMS. (c) Residual N_r (black) in ppmv with modified combustion efficiency overlaid (MCE, red).

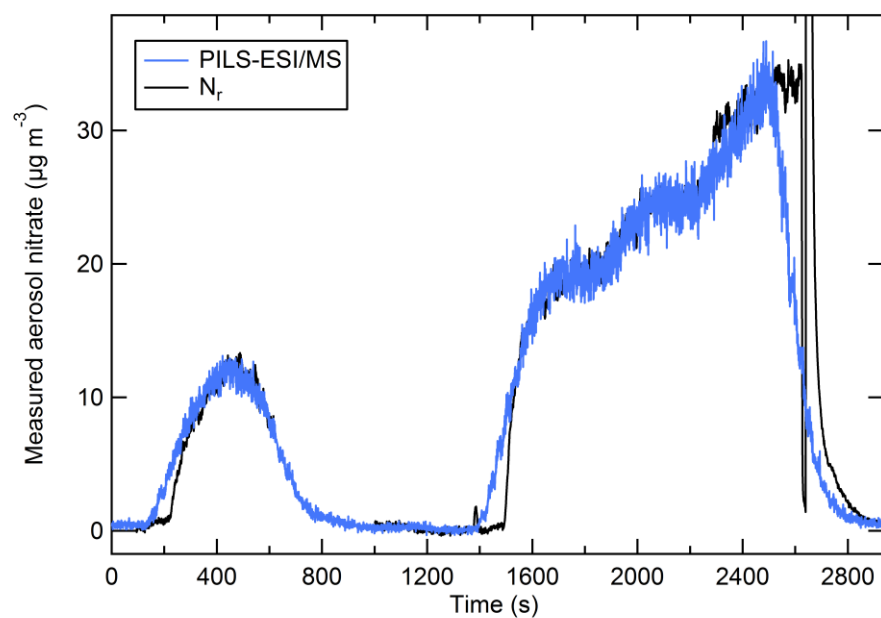


Figure 8. The PILS-ESI/MS measured aerosol nitrate mass (blue) and the nitrate measured as N_r (black) ($\mu\text{g m}^{-3}$) for an atomized solution of NaNO_3 (polydisperse). The PILS-ESI/MS trace is shifted to account for the delayed response and the instrument time constant.

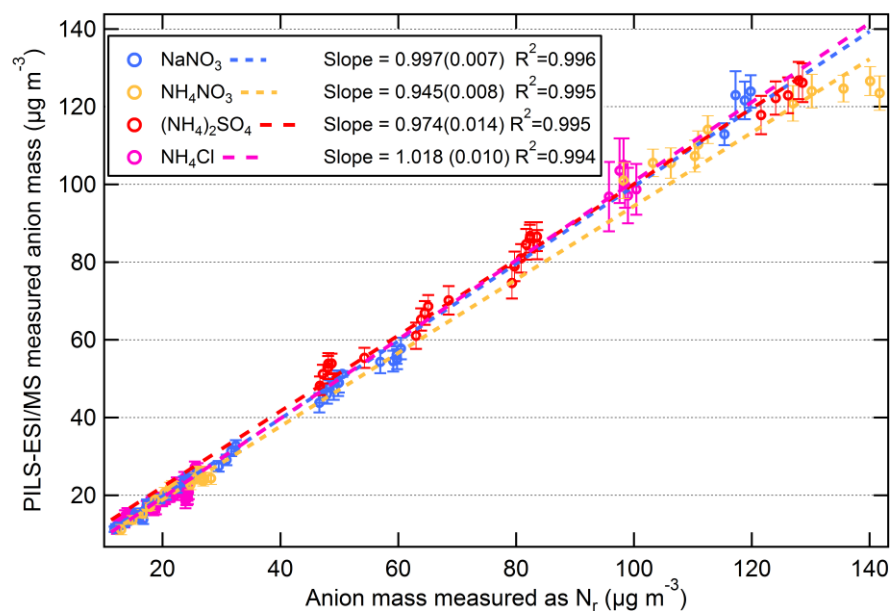


Figure 9. Scatter plots of PILS-ESI/MS measured versus equivalent anion mass measured as N_r for salts NaNO_3 (blue), NH_4NO_3 (gold), $(\text{NH}_4)_2\text{SO}_4$ (red), and NH_4Cl (magenta). The data are 60 s averages and only include times when the atomized aerosol output was relatively constant (i.e. not when concentrations were rising/falling). The slope (1σ) and R^2 is shown.

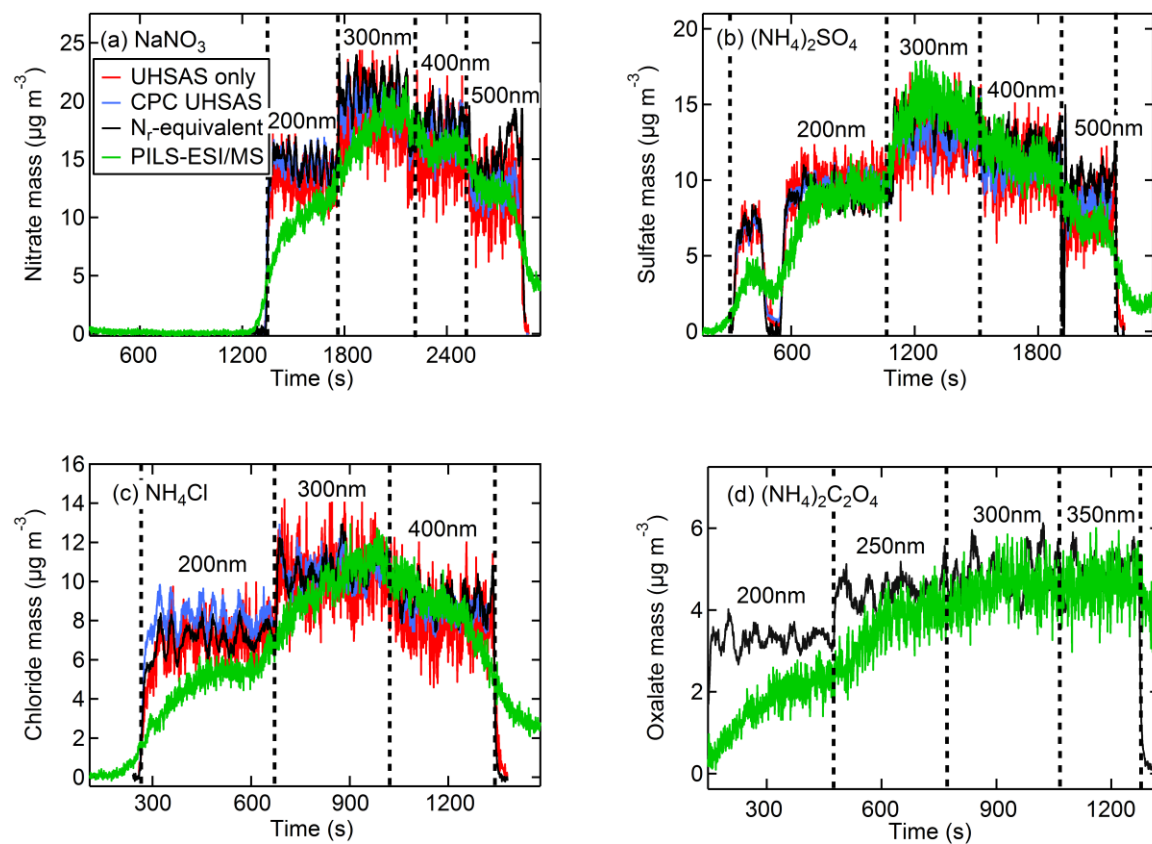


Figure 10. The N_r (black) measured, CPC number with UHSAS size (blue) calculated, UHSAS number and size (red) calculated, and PILS-ESI/MS (green) measured aerosol concentrations ($\mu\text{g m}^{-3}$) for anions of DMA size selected aerosol for salts of (a) NaNO_3 , (b) $(\text{NH}_4)_2\text{SO}_4$, (c) NH_4Cl , and (d) $(\text{NH}_4)_2\text{C}_2\text{O}_4$. The PILS-ESI/MS traces were shifted in time several minutes early to account for the delayed instrument response time.

Tables

Table 1. Conversion efficiencies of N_r compounds by the Pt/MoO_x catalyst system

Compound	Conversion efficiency (%)	Calibration method	Reference
Nitrogen Dioxide, NO ₂	99 ± 2	Titration of NO standard by O ₃	Williams et al., 1998
Ammonia, NH ₃	105-110 ± 15	Permeation tube or gas mixture, UV absorbance at 184.9nm	Neuman et al., 2003
Hydrogen cyanide, HCN	101-102 ± 10	Gravimetric gas mixture	GASCO, Oldsmar, FL.
Cyanogen chloride, ClCN	98 ± 10	Conversion of HCN standard with Chloramine-T	Valentour et al., 1974
Isocyanic Acid, HNCO	100 ± 25	Decomposition of the trimer, FTIR	Roberts et al., 2010
Nitrobenzene, C ₆ H ₅ NO ₂	95 ± 15	Liquid calibration unit, liquid flow and gravimetric concentration	Ionicon, Innsbruck, Austria
Triethyl amine, (C ₂ H ₅) ₃ N	95 ± 15	Liquid calibration unit, liquid flow and gravimetric concentration	Ionicon, Innsbruck, Austria

Table 2. Particle conversion efficiencies (%) with uncertainties (one standard deviation) in parentheses. The sizing accuracy is $\sim \pm 2.5\%$ using NIST-traceable PSLs for 150 –500 nm spheres as our calibration standard.

Diameter (nm)	NaNO₃	(NH₄)₂SO₄	NH₄Cl	(NH₄)₂C₂O₄
100	88.4(18.3)	100.6(3.0)	89.2(5.9)	91.0(3.5)
150	94.0(10.9)	96.5(2.5)	93.4(4.7)	89.0(6.6)
200	98.6(4.0)	98.8(4.8)	93.6(4.2)	90.2(5.1)
250	101(3)	100(3)	98.3(3.7)	94.7(5.6)
300	104(6)	102(9)	101(3)	97.0(6.2)
350	102(6)	101(9)	98.5(5.2)	101(13)
400	103(8)	100(8)	100(6)	94.7(7.4)
450	95.1(4.5)	110(4)	103(6)	-
500	103(15)	109(17)	124(11)	96.3(7.6)
600	83.2(8.7)	91.9(5.5)	-	82.5(8.4)
Average	97.3(7.1)	101(5)	100(10)	92.9(5.4)